Article:
Wang, F, Wu, N, Zhang, L et al. (9 more authors) (2018) Light Signaling-dependent Regulation of Photoinhibition and Photoprotection in Tomato. Plant Physiology, 176 (2). pp. 1311-1326. ISSN 0032-0889

https://doi.org/10.1104/pp.17.01143

Plant Physiology Preview. Published on November 16, 2017, as DOI:10.1104/pp.17.01143

1 **Running Title: HY5 in photoinhibition and photoprotection**

2

3 **Corresponding author:**

4 Yanhong Zhou

5 Department of Horticulture, Zijingang Campus, Zhejiang University, 866 Yuhangtang Road,

6 Hangzhou 310058, China.

7

8 Telephone: 0086-571-88982276

9 Fax: 0086-571-86971498

10 E-mail address:yanhongzhou@zju.edu.cn

11

12 **Research area:** Plant science and Ecology

Title: Light Signaling-dependent Regulation of Photoinhibition and Photoprotection in Tomato

Authors: Feng Wang[1], Nan Wu[1], Luyue Zhang[1], Golam Jalal Ahammed[1], Xiaoxiao Chen[1], Xun Xiang[1], Jie Zhou[1], Xiaojian Xia[1], Kai Shi[1], Jingquan Yu[1,2], Christine H. Foyer[3], and Yanhong Zhou[1,2,*]

[1]*Department of Horticulture, Zijingang Campus, Zhejiang University, 866 Yuhangtang Road, Hangzhou, 310058, P.R. China*

[2]*Zhejiang Provincial Key Laboratory of Horticultural Plant Integrative Biology, 866 Yuhangtang Road, Hangzhou, 310058, P.R. China*

[3]*Centre for Plant Sciences, Faculty of Biology, University of Leeds, Leeds, LS2 9JT, UK*

One sentence summary: Far-red light alleviates cold-induced photoinhibition and enhances photoprotection in shade leaves via activation of phyA-dependent HY5-ABI5-RBOH1 signaling pathways.

Footnotes:

List of author contributions

Author contributions

Y.Z. conceived the study and analyzed the data; F.W., N.W., L.Z., and X.C. performed the experiments; G.A., X.X., J.Z., Xi.X., and K.S. discussed the data; Y.Z., J.Y. and C. H. F wrote the article with contributions from the other authors.

Funding information: This work was supported by the National Natural Science Foundation of China (grant nos. 31672198, 31430076), the Fundamental Research Funds for the Central Universities (2016XZZX001-07) and the Fok Ying-Tong Education Foundation (132024).

*Corresponding author; email yanhongzhou@zju.edu.cn

ACKNOWLEDGMENTS

We are grateful to Prof. Jim Giovannoni of Cornell University and the Tomato Genetics Resource Center at the California University for tomato seeds. We thank Prof. Gang Lu (Zhejiang University) for denoting the CRISP/Cas9 vectors.

ABSTRACT

Photoreceptor-mediated light signaling plays a critical role in plant growth, development, and stress responses but its contribution to the spatial regulation of photoinhibition and photoprotection within the canopy remains unclear. Here, we show that low red/far-red (L-R/FR) ratio light conditions significantly alleviate PSII and PSI photoinhibition in the shade leaves of tomato plants. This protection is accompanied by a phytochrome A (phyA)-dependent induction of LONG HYPOCOTYL 5 (HY5). HY5 binds to the promoter of *ABA INSENSITIVE* 5 (*ABI5*), triggering *RESPIRATORY BURST OXIDASE HOMOLOG1* (*RBOH1*)-dependent H_2O_2 production in the apoplast. Decreased levels of *HY5, ABI5* and *RBOH1* transcripts increased cold-induced photoinhibition and abolished L-R/FR-induced alleviation of photoinhibition. L-R/FR illumination induced non-photochemical quenching (NPQ) of chlorophyll *a* fluorescence and increased the activities of Foyer-Halliwell-Asada cycle enzymes and cyclic electron flux (CEF) around PSI. In contrast, decreased *HY5, ABI5* and *RBOH1* transcript levels abolished the positive effect of L-R/FR on photoprotection. Loss of *PROTON GRADIENT REGULATION5* (*PGR5*)-dependent CEF led to increased photoinhibition and attenuated L-R/FR-dependent NPQ. These data demonstrate that HY5 is an important hub in the cross-talk between light and cold response pathways, integrating ABA and reactive oxygen species signaling leading to the attenuation of photoinhibition by enhanced induction of photoprotection in shade leaves.

INTRODUCTION

Low temperatures are a major factor limiting the productivity and geographical distribution of plant species. Tropical and subtropical plants are generally sensitive to chilling because of lack of the capacity for cold acclimation (Zhu et al., 2007). Many economically important species such as maize, rice and tomato are unable to survive long term exposures of temperatures below 12 °C. In addition to interspecific differences in chilling sensitivity, the tolerance of a given species to low growth temperatures varies between organs and according to developmental stage. Within the canopy, the upper "sun", leaves often exhibit a higher sensitivity to chilling than the shade leaves. However, little is known about the mechanisms that contribute to the spatial differences in chilling tolerance.

In many situations, leaves absorb more light than can be effectively utilized in photosynthesis, especially when plants are exposed to stress. The excess light energy has to be dissipated because over-excitation has the potential to damage the photosynthetic machinery, particularly PSII in the process called photoinhibition (Kingston-Smith et al., 1997; Kingston-Smith and Foyer, 2000; Foyer et al., 2017). This process is characterized by the decreases in the maximal photochemical efficiency of PSII (Fv/Fm) and in maximal P700 oxidation ($\Delta P700_{max}$) in PSI. Meanwhile, plants have evolved a range of photoprotective mechanisms to decrease the probability of damage to the PSII and PSI reaction centers. Photoprotection involves diverse processes such as chloroplast avoidance movement, dissipation of absorbed light energy as thermal energy (NPQ), pseudocyclic electron flow coupled to reactive oxygen species (ROS) scavenging systems (Foyer-Halliwell-Asada cycle), cyclic electron flow (CEF) around PSI and the photorespiratory pathway (Takahashi and Badger, 2011). The dominant component of NPQ is the energy-dependent nonphotochemical quenching (qE), which is induced by an increase in the proton gradient across the thylakoid membrane (ΔpH) under excess light conditions (Munekage et al., 2004). PSII subunit S (PsbS) protein acts as a sensor of lumen pH and may activate qE through conformational changes of LHCII (Li et al., 2002; Ahn et al., 2008). The mechanisms that contribute to NPQ are not completely understood but it is widely accepted that two distinct xanthophyll-dependent quenching mechanisms involving xanthophyll cycle

103 pigments and lutein 1, respectively, participate in the ΔpH-triggered, PsbS-mediated
104 conformational changes of LHCII (Ruban et al., 2007; Ahn et al., 2008). In the xanthophyll
105 cycle, violaxanthin (V) is converted into zeaxanthin (Z) under high light, via the
106 intermediate antheraxanthin (A), a reaction that is catalyzed by the enzyme violaxanthin
107 deepoxidase (VDE). The presence of Z activates thermal dissipation of the excess energy
108 (Niyogi et al., 1997, 1998). The de-epoxidation state of the xanthophyll cycle pigments is
109 thought to regulate qE-dependent NPQ (Kromdijk et al., 2016). Alterations in VDE activity
110 influence the extent of PSII photoinhibition (Niyogi et al., 1998; Han et al., 2010).

111 CEF around PSI is considered to involve NAD(P)H dehydrogenase (NDH) complex-
112 dependent and *PROTON GRADIENT REGULATION5* (*PGR5*)/*PGRL1* complex-dependent
113 pathways (Shikanai, 2007), the latter being responsible for most of the required additional
114 ΔpH generation across the thylakoid membrane (Munekage et al., 2004). The generation of
115 an increased trans-thylakoid ΔpH gradient by CEF is important for the activation of qE
116 (Munekage et al., 2004). *PGR5-PGRL1* dependent CEF pathway is regulated by the
117 chloroplastic redox state and is activated under stress conditions (Okegawa et al., 2008;
118 Strand et al., 2015). Decreases in both CEF and qE resulted in an inhibition of the synthesis
119 of the D1 protein (Takahashi et al., 2009). Moreover, loss of function of proteins involved in
120 CEF around PSI increased the sensitivity of plants to photoinhibition of PSII and also PSI
121 (Munekage et al., 2002). Furthermore, suppression of Foyer-Halliwell-Asada cycle enzymes
122 increased photoinhibition whilst an overexpression of the genes encoding these enzymes
123 tended to decrease photoinhibiiton (Foyer et al., 1995; Maruta et al., 2010).

124 The effects of high light intensities or fluctuations in light intensity on the extent of
125 photoinhibition of PSII and PSI have been intensively studied over the past 40 years (Kim
126 and Tokura, 1995). In contrast, relatively little is known about the effects of light quality on
127 photoinhibition or photoprotection. Plants have developed a set of sophisticated
128 photoreceptors, including phytochromes (PHYs), cryptochromes (CRYs), phototropins
129 (PHOTs) and UV-B light photoreceptors (e.g. UVR8) to perceive changes in light quality
130 (Möglich et al., 2010). Of these, blue-light photoreceptors (e.g. PHOT) have been reported
131 to activate chloroplast avoidance movements in sessile plants under excess light conditions
132 (Kasahara et al., 2002). Energy dissipation in green algae is also controlled by the PHOT

133 and UVR8 photoreceptors, which are activated by blue and UV light (Petroutsos et al., 2016;
134 Allorent et al., 2016; Allorent and Petroutsos, 2017). PhyA and phyB, which are the
135 photoreceptors for far-red light (FR) and red light (R) respectively, play a central role in
136 regulating the expression of a large number of light-responsive genes that are involved in
137 regulation of a wide range of processes from photomorphogenesis to stress responses (Quail,
138 2002a, 2002b; Franklin and Quail, 2010; Wang et al., 2016), however, the role of
139 phytochromes in the regulation of photoinhibition has not been well characterized. LONG
140 HYPOCOTYL 5 (HY5), a basic leucine zipper (bZIP) transcription factor, acts downstream
141 of multiple photoreceptors, in the signal transduction pathway that links various signaling
142 pathways including light and phytohormone signaling (Cluis et al., 2004; Jiao et al., 2007;
143 Lau and Deng, 2010). HY5 is also important in the regulation of cold acclimation responses,
144 promoting the expression of a large number of cold-inducible genes (Catala et al., 2011).
145 Interestingly, low temperatures lead to the stabilization of HY5 through exclusion of
146 CONSTITUTIVE PHOTOMORPHOGENIC1 (COP1) from the nucleus. COP1 is an E3
147 ubiquitin ligase targeting HY5 for proteasome-mediated degradation in response to light
148 (Catala et al., 2011). Whether HY5 is involved in the regulation of photoprotection and
149 photoinhibition is as yet unknown. However, HY5 is known to regulate the expression of
150 several ROS and anthocyanin-related genes (Catala et al., 2011).

151 Spatial variations in the chilling sensitivity of leaves at different positions in a canopy
152 have been reported under field conditions, the upper sun-exposed leaves being more easily
153 injured by a cold episode than the shade leaves. Shading not only decreases the light
154 intensity arriving the leaf surface, but also reduces the R/FR ratios of the light available to
155 the shade leaves (Sasidharan et al., 2009). However, the role of changes in R/FR ratio on
156 cold tolerance within a canopy remains largely unexplored, particularly with regard to
157 effects on photoinhibition and photoprotection. Here we show that spatial differences in
158 cold tolerance and in photoinhibition are linked to light-quality-regulated photoprotection.
159 Data are presented showing that low R/FR ratios induce an accumulation of *HY5* transcripts
160 in a phyA-dependent manner. The increased expression of *HY5* leads to improved cold
161 tolerance by enhancing ABA signaling through direct binding of HY5 to the *ABI5* promoter
162 and induction of *RBOH1*-dependent apoplastic H_2O_2 generation. ABI5 participates in the

163 regulation of photoprotection by inducing a strong antioxidant response, as well as
164 enhancing *PGR5*-dependent NPQ. Taken together, these data show that phytochrome-
165 mediated HY5-ABA-ROS signaling plays a key role in avoiding cold-induced
166 photoinhibition by inducing photoprotection within the canopy in response to variations in
167 light quality.
168

169 **RESULTS**

170 **Spatial Variation in Photoinhibition is Partially Attributable to the Changes in Light**
171 **Quality Conditions**

172 Tomato plants were grown to the 11th leaf-stage and then exposed to a cold treatment at
173 4 °C under white light for 7 d. The degree of photoinhibition of PSII and PSI was then
174 compared in leaves at the 9th and 5th ranks from the base. Leaves at the 9th rank had lower
175 Fv/Fm ratios and lower maximum P700 photooxidation level ($\Delta P700_{max}$), together with
176 higher levels of relative electrolyte leakage (REL) than the 5th leaves (Fig. 1, A and B;
177 Supplemental Fig. S1). Light quality analysis revealed that the R/FR ratio was decreased
178 from 1.3 at the 9th leaf rank to 0.5 at 5th leaf rank.

179 We then examined the effects of light quality on cold-induced photoinhibition by
180 exposing tomato plants at the 6-leaf stage to a cold treatment at 4 °C under high R/FR ratio,
181 i.e. low FR intensity (L-FR, 133 µmol m^{-2} s^{-1}) or low R/FR ratio, i.e. high FR intensity (H-
182 FR, 400 µmol m^{-2} s^{-1}) light conditions, respectively, using monochromatic LEDs. In these
183 experiments, the R light intensity was maintained at 200 µmol m^{-2} s^{-1} under both light
184 quality treatment regimes. Chilling-induced decreases in Fv/Fm ratios and in $\Delta P700_{max}$ were
185 lower under H-FR than the values determined in plants exposed to the L-FR conditions (Fig.
186 1, C and D; Supplemental Fig. S2, A and B). NPQ values, PsbS protein accumulation and
187 de-epoxidation state of the xanthophyll cycle, i.e. (A+Z)/(V+A+Z) ratio, were increased
188 after cold stress, especially under H-FR light conditions (Supplemental Fig. S2, C-E).
189 Western Blot analysis revealed that chilling stress induced a decrease in the accumulation of
190 the PsaB and PsaC proteins, especially under L-FR conditions (Fig. 1E). We also tested the
191 acceptor-side limitation in chilled leaves by application of 25 µM methyl viologen (MV).
192 Results showed that chilling-induced decrease of $\Delta P700_{max}$ was mostly relieved in the MV-
193 treated leaves, especially under H-FR conditions (Fig. 1F). These results suggest that the
194 main cause of the chilling-induced decrease in $\Delta P700_{max}$ is the degradation of PSI submits
195 resulting in an acceptor side limitation in PSI.

196 RNA-seq analysis was performed on the 4th leaves after exposure of plants to a cold
197 treatment at 4 °C under either L- or H- FR light conditions. This generated a total of
198 103,463,126 reads, which were aligned to the *Solanum lycopersicum* reference genome

199 (https://solgenomics.net/). Compared with the plants grown under L-FR conditions, a total
200 of 6312 transcripts (3607 increased in abundance and 2705 decreased in abundance) were
201 differentially changed under the H-FR (Supplemental Table S1). An examination of the
202 levels of transcripts encoding photosynthetic proteins, and proteins involved in light and
203 ABA signaling revealed a subset of mRNAs that showed differential changes in response to
204 the light quality, having higher levels in leaves exposed to H-FR light compared to L-FR.
205 These transcripts encoded proteins are involved in PSII (*PHOTOSYSTEM II LIGHT*
206 *HARVESTING COMPLEX GENE 2.1* and *PHOTOSYSTEM II REACTION CENTER*
207 *PROTEIN A*), PSI (*PHOTOSYSTEM I SUBUNIT I* and *PHOTOSYSTEM I, PsaA/PsaB*
208 *PROTEIN*), cyclic electron flux (*PGR5* and *PGR5-LIKE A*), plastoquinone cytochrome b_6f
209 comples (*CYTOCHROME b561/FERRIC REDUCTASE TRANSMEMBRANE PROTEIN*
210 *FAMILY* and *CYTOCHROME B5 ISOFORM B*), FAD/NAD(P)-binding oxidoreductase
211 family protein (*NAD(P)-BINDING ROSSMANN-FOLD SUPERFAMILY PROTEIN* and
212 *FAD/NAD(P)-BINDDING OXIDOREDUCTASE FAMILY PROTEIN*), oxidoreductase
213 proteins (*PEROXIDASE 2* and *ASCORBATE PEROXIDASE 3*), thermal energy dissipation
214 (*CAROTENOID CLEAVAGE DIOXYGENASE 1* and *ZEAXANTHIN EPOXIDASE, ZEP*;
215 Supplemental Fig. S2F; Supplemental Table S2).
216

217 **PhyA Acts as a Positive Regulator for Light Quality-Dependent Regulation of**
218 **Photoinhibition**

219 Cold-induced photoinhibition was compared in wild type (WT) tomato leaves and in
220 mutants deficient in phytochrome A (*phyA* and *phyAB1B2*) or phytochrome B (*phyB1B2*)
221 grown under either L-FR or H-FR conditions. The *phyA* mutants had lower Fv/Fm ratios
222 and $\Delta P700_{max}$ levels than the WT following exposure to a cold treatment at 4 °C for 7 d (Fig.
223 2A). In contrast, the *phyB1B2* plants showed higher Fv/Fm ratios and $\Delta P700_{max}$ values than
224 the WT under these conditions. Moreover, the *phyA* and *phyAB1B2* mutants had lower NPQ
225 values, with less PsbS protein accumulation and lower CEF rates compared to WT plants
226 (Fig. 2, B-D). In contrast, the *phyB1B2* plants had higher NPQ values, PsbS protein
227 accumulation and CEF rates than the WT. In addition, H-FR significantly induced increases
228 in Fv/Fm ratios, $\Delta P700_{max}$ values, NPQ values, PsbS protein accumulation and CEF rates in

229 WT and *phyB1B2* mutant, but not in *phyA* and *phyAB1B2* mutants after the cold treatment
230 (Fig. 2, A-D).
231 The levels of *HY5* transcripts were increased in response to a cold treatment in WT
232 tomato leaves grown under H-FR compared to L-FR conditions (Fig. 2E). The H-FR growth
233 regime also resulted in significant chilling-induced increases in the levels of *HY5* transcripts
234 in the *phyB1B2* mutant leaves but not in those of the *phyA* or *phyAB1B2* mutants. However,
235 an inverse pattern of response to change in FR intensity was observed for *COP1* transcripts.
236 Growth under the H-FR light regime decreased the levels of *COP1* mRNAs in the WT and
237 in the *phyB1B2* mutants under cold stress. In contrast, differences in the FR intensity had
238 little effect on the levels of *COP1* transcripts in *phyA* and *phyAB1B2* mutants after the cold
239 treatment.
240
241 **FR-Induced HY5 Alleviated Photoinhibition by Induction of Photoprotection**
242 The levels of *HY5* and *COP1* transcripts were decreased by 80% and 70%, respectively,
243 in *HY5*-RNAi and *COP1*-RNAi plants used for the study (Supplemental Fig. S3A). Cold
244 and FR intensity-induced changes in Fv/Fm ratios, $\Delta P700_{max}$, survival rates, REL and the
245 levels of oxidized protein, as determined by the presence of protein carbonyl groups, were
246 measured in the *HY5*-RNAi and *COP1*-RNAi plants (Fig. 3, A and B; Supplemental Fig. S3,
247 B and C). Cold-induced increases in REL and in the levels of oxidized proteins were higher
248 in the *HY5*-RNAi plants compared to the WT and *COP1*-RNAi plants regardless of FR
249 intensity (Supplemental Fig. S3C). In contrast, the Fv/Fm ratios and the $\Delta P700_{max}$ values
250 were much lower in the leaves of the *HY5*-RNAi plants compared to the WT and *COP1*-
251 RNAi plants under both FR light conditions (Fig. 3, A and B). The chilling-induced
252 decreases in the Fv/Fm ratios and the $\Delta P700_{max}$ values were significantly less in the *COP1*-
253 RNAi plants than the WT (Fig. 3, A and B). Significantly, H-FR treatment induced
254 increases in Fv/Fm ratios, $\Delta P700_{max}$ values, survival rates and decreases in REL or the
255 levels of oxidized proteins in the WT and the *COP1*-RNAi plants, but had little effects on
256 these parameters in the *HY5*-RNAi plants (Fig. 3, A and B; Supplemental Fig. S3, B and C).
257 Moreover, the *HY5*-overexpressing plants showed an increased tolerance to the cold
258 treatment compared to the WT (Supplemental Fig. S4). Taken together, these results

259 indicate that HY5 is required for the light quality-mediated regulation of chilling tolerance
260 in tomato and that COP1 negatively regulates this process.

261 NPQ, cyclic electron flux (CEF) and Foyer-Halliwell-Asada cycle all play important
262 roles in preventing the photosystems from photodamage or photoinhibition (Foyer et al.,
263 1995; Takahashi et al., 2009; Chen and Gallie, 2012). In comparison to the WT plants, the
264 *HY5*-RNAi plants showed decreased levels of NPQ, PsbS protein accumulation, antioxidant
265 enzyme activities and CEF rates (Fig. 3, C-F; Supplemental Fig. S5). These parameters were
266 increased in the *COP1*-RNAi plants relative to the WT. An increase in the FR intensity
267 significantly increased the level of NPQ and the accumulation of PsbS protein, and the
268 abundance of transcripts encoding Foyer-Halliwell-Asada cycle enzymes (*Cu/Zn-*
269 *SUPEROXIDE DISMUTASE, Cu/Zn-SOD*; *ASCORBATE PEROXIDASE, tAPX*;
270 *MONODEHYDROASCORBATE REDUCTASE, MDAR*; *DEHYDROASCORBATE*
271 *REDUCTASE, DHAR* and *GLUTATHIONE REDUCTASE 1, GR1*), as well as the activities
272 of these enzymes, and the rate of CEF in WT and *COP1*-RNAi plants (Fig. 3, C-F;
273 Supplemental Fig. S5). The effects of the FR intensity were more pronounced in the *COP1*-
274 RNAi plants. However, the H-FR treatment had little effect on the level of NPQ, the
275 activities of antioxidant enzymes or the rates of CEF in the *HY5*-RNAi plants, suggesting
276 that HY5 is essential for the H-FR regulation of photoprotection.
277

278 **HY5 is a Transcriptional Activator of *ABI5***

279 While exposure to cold stress had no effect on stomatal movements in *HY5*-RNAi
280 plants, this treatment caused a decrease in stomatal aperture in *COP1*-RNAi leaves,
281 especially under H-FR light conditions (Supplemental Fig. S6, A and B). Given that ABA
282 signaling positively regulates stomatal movement, we examined whether HY5 could bind to
283 the promoters of any of the ABA signaling genes. For this analysis, we inspected 2.5 kb
284 sequences upstream of the transcriptional start sites of a set of tomato *ABA INSENSITIVE*
285 (*ABI*) genes. Of these, the promoters of three ABA signaling genes (*ABI3-1, ABI3-2* and
286 *ABI5*) contain the G-box sequences: CACGTG (Fig. 4A; Supplemental Fig. S6C).
287 Electrophoretic mobility shift assays (EMSA) were used to analyze whether HY5 binds
288 directly to these promoters *in vitro*. The probe-protein complex was not detected using

289 *ABI3-1* and *ABI3-2* probes. However, HY5 directly bound to the promoter probe of *ABI5*
290 (Fig. 4C; Supplemental Fig. S6D). When the core sequence of G-box element motif in *ABI5*
291 probe was mutated in a single base (*ABI5-G-mut2*) or multiple bases (*ABI5-G-mut1*, Fig.
292 4B), the binding to the complexes was decreased, or even totally lost (Fig. 4C). Based on
293 these observations, we conclude that HY5 protein binds specifically to the G-box element
294 sequences of the synthesized probes for the *ABI5* promoters *in vitro*.

295 To further determine whether the tomato HY5 protein binds directly to the promoter of
296 *ABI5 in vivo* under cold stress, we performed ChIP-qPCR assays. As shown in Fig. 4D, the
297 *ABI5* promoter sequence was substantially enriched in fractions using the anti-HA antibody
298 that immune-precipitates the 3HA-tagged HY5 transgene product in the *HY5* overexpressing
299 (OE) lines but not the WT after 6 h of cold stress under H-FR. However, the IgG control
300 antibody failed to pull down *ABI5* gene promoter DNA segment (Fig. 4D). We then
301 assessed the levels of *ABI5* transcripts in WT, *HY5*-RNAi and *COP1*-RNAi plants exposed
302 to H- and L-FR conditions under cold stress conditions (Fig. 4E). No changes in *ABI5*
303 transcript levels were detected in the *HY5*-RNAi plants in relation to the FR intensity. In
304 contrast, an increase in the FR gradually induced increase the abundance of *ABI5* transcripts
305 in WT and *COP1*-RNAi plants, the induction being more significant in the *COP1*-RNAi
306 plants than the WT. The induction of *ABI5* expression was greater in the *HY5*
307 overexpressing lines (OE#1 and OE#3, expressing high HY5 protein levels, Supplemental
308 Fig. S4A) than the WT after 6 h of cold stress under the H-FR irradiance regime (Fig. 4F).
309 These results indicate that HY5 binds directly the promoter of *ABI5* and activates its
310 expression, subsequently regulates cold tolerance of tomato in response to light quality.

311 When WT and phytochrome mutant plants were exposed to L-FR and H-FR light
312 conditions at 4 °C, higher levels of *ABI5* transcripts were maintained in *phyB1B2* mutants
313 compared to the WT, *phyA* or *phyAB1B2* plants under both light quality conditions (Fig. 4G).
314 Moreover, the higher FR intensity increased the levels of *ABI5* transcripts in WT and
315 *phyB1B2* plants, but not in *phyA* or *phyAB1B2* mutants.

316

317 **Role of *ABI5* in Light Quality-Regulated Photoinhibition and Photoprotection**

318 Lines of *ABI5*-silenced (pTRV-*ABI5*) plants were generated, using a virus-induced
319 gene silencing (VIGS). These lines showed a reduction in *ABI5* transcript levels of 75%
320 (Supplemental Fig. S7, A and B). Tomato pTRV-*ABI5* plants showed an increased
321 sensitivity to cold-induced photoinihibition compared to the pTRV plants, as measured by a
322 decrease in the Fv/Fm ratio and in $\Delta P700_{max}$, as well as an increase in REL (Fig. 5, A and B;
323 Supplemental Fig. S7, C and D). Interestingly, the H-FR-induced cold tolerance and
324 alleviation of photoinhibition observed in the pTRV plants was completely lost in the *ABI5*-
325 silenced plants, which showed no significant differences in Fv/Fm ratios, $\Delta P700_{max}$ under
326 cold stress at both light quality regimes. These observations clearly indicate that loss of
327 *ABI5* function compromised the H-FR-induced alleviation of chilling dependent
328 photoinhibition in tomato. In support of this hypothesis, we observed that the H-FR-induced
329 changes in NPQ, PsbS protein accumulation, and the activities of antioxidant enzymes, as
330 well as the rate of CEF were abolished or attenuated in the pTRV-*ABI5* plants (Fig. 5, C-F).
331 These results show that *ABI5* functions as a down-stream of HY5 in light-regulated
332 photoprotection.
333
334 ***RBOH1*-Dependent ROS Production Prevents Photoinhibition by Activation of**
335 **Photoprotection**
336 ABA signaling is linked to the upregulation of RBOH-dependent ROS production in
337 response to stress (Murata et al., 2001; Xing et al., 2008; Zhou et al., 2014). The cold
338 treatment used in the present study increased the levels of *RBOH1* transcripts and apoplastic
339 H_2O_2 accumulation (Fig. 6, A and B). Moreover, silencing *ABI5* (pTRV-*ABI5*) abolished the
340 H-FR-dependent induction of *RBOH1* expression and apoplastic H_2O_2 accumulation.
341 *RBOH1*-RNAi plants were used to examine whether *RBOH1* plays a role in the
342 regulation of cold-induced photoinhibition and photoprotection under L- and H-FR
343 conditions. The *RBOH1*-RNAi plants showed lower apoplastic H_2O_2 accumulation and an
344 increased sensitivity to photoinhibition compared to the WT. The response to changes in FR
345 intensities was also compromised in terms of survival rates and changes in the Fv/Fm ratios,
346 $\Delta P700_{max}$ and REL (Fig. 6, C and D; Supplemental Fig. S8). In addition, ABA-induced
347 alleviation of photoinihibition was compromised by treatment with dimethylthiourea

348 (DMTU, a ROS scavenger). This effect was also not observed in the *RBOH1*-RNAi plants
349 (data not shown). Moreover, H-FR-induced changes in NPQ, PsbS protein accumulation and
350 the activities of antioxidant enzymes, as well as the rate of CEF were abolished in the
351 *RBOH1*-RNAi plants (Fig. 6, E-H). These results suggest that the *ABI5*-dependent
352 production of H_2O_2 plays a pivotal role in HY5-regulated photoprotection by functioning as
353 a critical downstream component in light signaling.
354
355 **Light-Activated CEF Plays Dual Roles in Preventing Plants from Photoinhibition**
356 The roles of NPQ and antioxidants in photoprotection are well established (Foyer et al.,
357 1995; Niyogi et al., 1997, 1998; Chen and Gallie, 2012). However, relatively, little is known
358 about the role of PGR5-PGRL1-dependent and NDH-dependent CEF in photoprotection
359 (Shikanai, 2007). Here, we show that chilling stress increased the accumulation of *PGR5*
360 transcripts by more than 5-fold but had less effect on the levels of *PGRL1A* and *ORANGE*
361 *RIPENING* (*ORR*) transcripts (Supplemental Fig. S9). *ORR* encodes an NDH-M subunit in
362 the tomato Ndh complex (Nashilevitz et al., 2010). Chilling-induced increases in *PGR5*,
363 *PGRL1A* and *ORR* transcripts were greater following exposure of plants to H-FR light
364 conditions. In comparison, *PGRL1B* transcripts were decreased by the chilling treatment and
365 they were not affected by FR levels. Moreover, *PHYA* deficiency or silencing of *HY5, ABI5*
366 and *RBOH1* abolished the H-FR-dependent induction of *PGR5*, *PGRL1A* and *ORR*
367 transcripts. These results suggested the potential involvement of the PGR5-PGRL1
368 dependent and NDH dependent CEF in the photoprotection in response to the cold stress.
369 We then generated *pgr5* mutants by using a Crisp/cas9 technique and also *PGR5*-
370 overexpressing (*PGR5*-OE) tomato plants (Supplemental Fig. S10). The *pgr5* plants showed
371 decreased CEF rates while the *PGR5*-OE plants had increased CEF rates under cold stress
372 (Supplemental Fig. S11C). Moreover, the cold-mediated induction of CEF under H-FR light
373 conditions was lower in the *pgr5* plants than the WT. In contrast, this parameter was higher
374 in the *PGR5*-OE plants exposed to cold stress under H-FR light conditions. Significantly,
375 the cold treatment led to greater decreases in the Fv/Fm ratios and in $\Delta P700_{max}$, and in
376 increase in REL in the *pgr5* plants than the WT (Fig. 7, A and B; Supplemental Fig. S11, A
377 and B), while *PGR5*-overexpressing significantly increased Fv/Fm ratios and $\Delta P700_{max}$

378 values after a cold stress. H-FR induced increases in qE, NPQ, PsbS protein acclimation and
379 (A+Z)/(V+A+Z) ratio in the WT and *PGR5*-OE plants but not in the *pgr5* plants (Fig. 7, C-
380 F). These results suggest that PGR5-dependent CEF is essential for light-regulated
381 photoprotection. To provide further evidence for the roles of *HY5*, *ABI5* and *RBOH1* in
382 PGR5-dependent photoprotection, we silenced *HY5*, *ABI5* and *RBOH1* in *PGR5*-OE plants
383 (Supplemental Fig. S12). As observed in WT plants, silencing of these genes in *PGR5*-OE
384 plants significantly decreased $\Delta P700_{max}$ and compromised H-FR-induced increase in
385 $\Delta P700_{max}$. These findings show that HY5-ABI5-RBOH1 cascades play a critical role in FR-
386 induced and PGR5-dependent photoprotection in the plants.
387
388 **DISCUSSION**
389 The management of light energy usage in photosynthesis is a key concept of
390 photosynthetic regulation (Foyer et al., 2017). A wide range of mechanisms have evolved to
391 protect the photosystems from the potentially damaging effects of the high irradiances that
392 occur in the natural environments. While photoinhibition may not be such a common
393 phenomenon in nature as was once thought because recovery without damage is facilitated
394 by the protective component of NPQ (Foyer et al., 2017), understanding the regulation of
395 NPQ at different leaf ranks within the plant canopy is crucial to plant productivity. The
396 recent demonstration that acceleration of the NPQ relaxation can lead to significant
397 increases in crop yield (Kromdijk et al., 2016), highlights the importance of understanding
398 how photosynthetic efficiency is regulated. The data presented here provides new
399 information concerning the regulation of leaves to shading. We show that spatial variations
400 in susceptibility to cold-induced photoinhibition are attributable to differences in the R/FR
401 ratios experienced by the leaves. In particular, phyA-mediated induction of *HY5* under
402 different R/FR regimes plays a critical role in photoprotection. Through binding to the
403 promoter of *ABI5*, HY5 triggers enhanced protoprotection through induction of an
404 apoplastic H_2O_2 burst that influences antioxidant status, CEF and NPQ. This enhanced
405 photoprotection allows shade leaves to avoid photoinhibition.
406 Chlorophyll-containing cells absorb blue light and R light, whereas FR photons are
407 either transmitted or reflected. This leads to a decrease in the R/FR ratios experienced deep

408 leaves within the vegetative canopy compared to leaves exposed to full sunlight (Sasidharan
409 et al., 2009). The data presented here show that the upper leaves experiencing a high R/FR
410 ratios (i.e. low FR intensity, L-FR) growth environment have a higher degree of
411 photoinhibition compared to shade leaves that experience a low R/FR ratios (i.e. high FR
412 intensity, H-FR) growth environment (Fig. 1, A and B; Supplemental Fig. S1). To exclude
413 the potential effects of other parameters such as leaf developmental stage and light intensity
414 on photoinhibition and cold tolerance, plants were exposed to R at same light intensity and
415 only FR intensities were changed. Photoinhibition and electrolyte leakage were significantly
416 decreased, while NPQ values, PsbS protein accumulation and (A+Z)/(V+A+Z) ratio were
417 increased under the low-R/FR ratios light growth regime (Fig. 1, C-F; Supplemental Fig. S2,
418 A-E). Therefore, spatial differences in sensitivity to photoinhibition and in cold tolerance
419 are largely attributable to differences in R/FR ratios within the growth environment.
420 Moreover, the low R/FR ratio experience by the leaves plays a positive role in tolerance to
421 excess light such that shade leaves are less sensitive to photoinhibition. By using western
422 blotting against PSI subunits PsaB and PsaC, and suppling of MV, an artificial electron
423 acceptor from PSI, we found FR plays a critical role in photoprotection by alleviating the
424 degradation of PSI submits and the release of acceptor side limitation of PSI (Fig. 1, E and
425 F).

426 It is widely accepted that the primary functions of phytochromes is to detect
427 environmental fluctuations in the relative proportions of R and FR radiation (Chen et al.,
428 2004). Data presented here show that the FR receptor phyA and R receptor phyB are
429 respectively, positive and negative regulators of photoinhibition (Fig. 2, A-D). These
430 findings are in agreement with earlier studies demonstrating that *phyA* and *phyB1B2*
431 deficient tomato plants had increased and decreased sensitivities to chilling (Wang et al.,
432 2016). It is of interest to note that the higher tolerance to cold observed in shade leaves
433 contrasts markedly with the reported decreased resistance to herbivory and pathogens.
434 Numerous studies have reported that the low R/FR ratios experienced by shade leaves
435 increase plant population densities, and increase herbivory and disease (Xie et al., 2011;
436 Ballaré, 2014). In contrast to the increases in cold tolerance observed here in *phyB* tomato
437 plants, similar mutants in Arabidopsis were reported to be more sensitive to *Pseudomonas*

438 *syringae* pv. *tomato* DC3000 (de Wit et al., 2013). Recent studies have demonstrated that
439 high R/FR ratios have important effects on plant defenses through effects on JA signaling
440 and other defense pathways (Cerrudo et al., 2012; Nagata et al., 2015). Therefore, plants
441 appear to have evolved different mechanisms for coping with biotic stress and abiotic
442 stresses through the integration of light signaling pathways with those involving the
443 perception of other environmental stimuli.

444 Multiple photoreceptors promote the accumulation of HY5 in response to changing light
445 conditions. As a member of the bZIP transcription factor family, HY5 plays a critical role in
446 different plant processes such as hormone-, nutrient-, abiotic stress- and redox-signaling
447 pathways (Gangappa and Botto, 2016). This places HY5 at the center of the transcriptional
448 network hub that regulates plant responses to environmental change. One mechanism by
449 which this is achieved is through regulation of the nuclear abundance of COP1, an E3
450 ubiquitin ligase that targets HY5 for proteasome-mediated degradation in darkness
451 (Osterlund et al., 2000; Yi and Deng, 2005). Exposure to cold stress induced *HY5*
452 expression in WT and *phyB1B2*. However, mutation in *phyA* abolished cold-induced
453 transcript of *HY5* under both L-FR and H-FR light conditions (Fig. 2E). In addition, changes
454 in the *COP1* transcript levels were in contrast with those in *HY5* transcript levels in WT
455 leaves and in phytochrome-deficient mutants. These results suggest that the induction of
456 *HY5* and *COP1* in response to the cold stress is phyA and phyB-dependent respectively. To
457 date, our knowledge of the role of HY5 in plant cold responses was limited to the regulation
458 of anthocyanin accumulation in Arabidopsis (Catala et al., 2011). The data presented here
459 show that HY5 and COP1 are positive and negative regulators for the plant cold response
460 leading to the regulation of photoinhibition (Fig. 3; Supplemental Figs. S3-S5).

461 ABA signaling is known to play an important role in responses to various
462 environmental stresses (Zhao et al., 2013). Analysis using EMSA and ChIP-qPCR assay
463 revealed that HY5 binds to the G-box element of the *ABI5* promoter *in vitro* and *in vivo* with
464 a high specificity (Fig. 4, A-D; Supplemental Fig. S6, C and D). In the absence of HY5, the
465 ability of H-FR-induced signals to increase *ABI5* transcript levels was impaired (Fig. 4E).
466 The induction of *ABI5* expression was also found to be phyA-dependent and significantly
467 increased in *HY5*-overexpressing plants compared to WT plants after exposure to cold stress

468 (Fig. 4, F and G). ABI5 had been shown to be involved in the regulation of seed germination
469 and responses to drought (Chen et al., 2008). ABI5 involvement in drought stress responses
470 has been assessed through adjustments in ROS scavenging and in osmotic potential in
471 cotton (Mittal et al., 2014). ABA signaling, like brassinosteroid signaling, is known to have
472 a role in the induction of aploplastic H_2O_2 accumulation in plants (Zhou et al., 2014). The
473 data presented here show that silencing *ABI5* compromised the H-FR-induced alleviation of
474 photoinhibition (Fig. 5; Supplemental Fig. S7), as well as the induction of *RBOH1*
475 expression and H_2O_2 accumulation in the leaf apoplast (Fig. 6, A and B). Taken together,
476 these findings strongly suggest that *ABI5* not only functions as a downstream component of
477 the light-regulated cold tolerance pathway in a HY5-dependent manner, but that it is also
478 linked to ROS signaling. Furthermore, *RBOH1*-RNAi plants failed to respond to changes in
479 FR intensities in terms of effects on Fv/Fm and $\Delta P700_{max}$ (Fig. 6, C-H; Supplemental Fig.
480 S8). These findings suggest that *RBOH1*-dependent H_2O_2 production plays an essential role
481 in the adjustment of the photosynthetic processes to changes in light quality. Taken together,
482 our results demonstrate that light quality signaling participates in the regulation of the
483 responses of photosynthesis to chilling by regulation of HY5-ABI5-RBOH1 signaling
484 pathways.

485 Plants absorb sunlight to power the photochemical reactions of photosynthesis with the
486 generation of ROS, a process that is increased under stress (Foyer et al., 2012). While ROS
487 are highly reactive and have been proposed to accelerate photoinhibition through direct
488 oxidative damage to PSII/PSI (Nishiyama et al., 2006), they are also vital signals relaying
489 information concerning changes in the redox status of the chloroplast to the nucleus stress
490 (Foyer et al., 2012). Plants have developed diverse photoprotection mechanisms to limit
491 light-induced damage to the photosynthetic apparatus (Takahashi and Badger, 2011).
492 Thermal energy dissipation, cyclic electron flow and the direct transfer of energy and
493 electrons to oxygen in pseudocyclic electron flow fulfill crucial roles in photosynthetic
494 regulation and photoprotection (Foyer et al., 2012). The data presented here show that the
495 increased sensitivity to cold-induced photoinhibition observed in the *HY5*-RNAi, pTRV-
496 *ABI5* and *RBOH1*-RNAi plants was linked to decreased capacity of photoprotection (Figs. 3,
497 5 and 6; Supplemental Figs. S3-5, 7 and 8). These findings suggest that the HY5-ABI5-

498 RBOH1 signaling pathway plays a critical role in the induction of the photoprotection
499 mechanisms that serve to avoid cold-induced photoinhibition.

500 The data presented here show that exposure to H-FR intensities induce NPQ, PsbS
501 protein accumulation and CEF, as well as increasing the activities of five enzymes involved
502 in antioxidant reactions in plants experiencing cold stress. Moreover, loss of *HY5*, *ABI5* or
503 *RBOH1* functions compromised the H-FR-induced NPQ, CEF and the increases in
504 antioxidant enzyme activities at low temperatures (Figs. 3, C-E, 5, C-F and 6, D-H;
505 Supplemental Fig. S5). We conclude that the HY5-ABI5-RBOH1 pathway is required for
506 the FR induction of photoprotection in response to cold stress. It is worth noting that *phyA*,
507 *HY5*-RNAi, pTRV-*ABI5* and *RBOH1*-RNAi plants all showed reduced accumulation of the
508 NPQ effector protein PsbS relative to WT and they showed little response to increases in FR
509 light intensities (Figs. 2D, 3E, 5E and 6G). Reduced accumulation of PsbS and the
510 insufficient trans-thylakoid ΔpH, caused by their severely damaged CEF may contribute to
511 the impaired NPQ in these plants (Figs. 2B-D, 3C-E, 5C-E and 6E-G). In addition, a FR-
512 induced increase in (A+Z)/(V+A+Z) ratios was not observed in these plants (data not
513 shown). It is plausible that the FR-activated and phyA-mediated HY5-ABI5-RBOH1-
514 dependent signaling pathway is linked to a NPQ-specific effect on photoprotection. While
515 transcript of *PGR5* was under the regulation by HY5, ABI5 and RBOH1 in response to the
516 change in FR intensity, silencing of *HY5, ABI5* and *RBOH1* in *PGR5*-OE plants also
517 compromised H-FR-induced increase in ΔP700max. (Supplemental Fig. S12). In this case,
518 ΔP700max was influenced by both the inherent *PGR5*, which could be modified by light
519 conditions, and 35S promoter driven *PGR5*, which is insensitive to the changes in light
520 conditions, respectively. This is why H-FR altered the ΔP700max in WT and *PGR5*-OE
521 plants to a similar degree. However, we could not exclude the possibility for the
522 involvement of other regulatory mechanisms. HY5 is also required for the suppression of
523 excessive ROS accumulation during acclimation to low temperatures (Catala et al., 2011).
524 Similarly, ABA signaling also plays a role in the expression and/or activities
525 of antioxidant enzymes, a role that is dependent to a large extent on the induction of
526 apoplastic H_2O_2 production (Zhang et al., 2007). We have previously reported that
527 apoplastic H_2O_2 production plays a critical role in cold acclimation by protection of PSII

528 (Zhou et al., 2012). Therefore, FR-induces photoprotection and suppresses excessive ROS
529 accumulation in a *HY5*-, *ABI5*- and *RBOH1*-dependnet manner. The role of SOD, APX,
530 MDAR, DHAR and GR as well as NPQ in photoprotection has been well established in
531 plants including tomato (Foyer et al., 1995; Chen and Gallie, 2012; Duan et al., 2012). The
532 results presented here show that PGR5-dependent CEF is important in photoprotection in
533 tomato leaves experiencing cold stress (Fig. 7; Supplemental Figs. S9-S12). Similar to the
534 apoplastic H_2O_2-dependent induction of the antioxidant response, the induction of CEF was
535 also shown to be dependent on apoplastic H_2O_2 production (Fig. 6E). These observations are
536 in agreement with earlier findings showing that H_2O_2 participates in the induction of CEF
537 (Strand et al., 2015; Guo et al., 2016). In agreement with the role of CEF in the activation of
538 ATP production and qE (Munekage et al., 2004; Guo et al., 2016; Yamori et al., 2016), we
539 show that loss of PGR5 functions in the *pgr5* mutant impaired H-FR-induced qE, NPQ,
540 PsbS protein accumulation and increases in (A+Z)/(V+A+Z) ratios (Fig. 7, C-F). These
541 results not only demonstrate the involvement of apoplastic H_2O_2 in the induction of ROS
542 scavenging, CEF and NPQ, but also emphasize the roles of CEF in photoprotection.
543

544 **MATERIALS AND METHODS**

545 **Plant Material and Growth Conditions**

546 Wild-type tomato (*Solanum lycopersicum*) cv 'Ailsa Craig' and cv 'Moneymaker', and
547 the *phyA, phyB1B2,* and *phyAB1B2* mutants in the cv Moneymaker background were
548 obtained from the Tomato Genetics Resource Center (http: //tgrc.ucdavis.edu). *HY5*-RNAi,
549 *COP1*-RNAi and *RBOH1*-RNAi plants were generated as described previously (Liu et al.,
550 2004; Guo et al., 2016). These transgenic plants were identified by resistance to Basta and
551 then by quantitative real-time (qRT)-PCR analysis for the transgene. For the generation of
552 *HY5* overexpressing transgenic plants, a 474 bp full-length *HY5* cDNA fragment was
553 obtained by RT-PCR using the primer pair *HY5*-OE-F with an *Asc*I site and *HY5*-OE-R with
554 a *Sal*I site (Supplemental Table S3). The PCR product was cloned into pFGC1008-HA
555 vector behind the CaMV 35S promoter to generate the *HY5*-OE-HA clone. The tobacco
556 rattle virus (TRV)-based vectors (pTRV1/2) were used for the virus-induced gene silencing
557 (VIGS) of tomato *HY5*, *ABI5* and *RBOH1* genes with the specific PCR-amplified primers

558 listed in Supplemental Table S3 (Liu et al., 2002). VIGS was performed as described
559 previously (Xia et al., 2014).
560 *PGR5* CRISPR/Cas9 vector was constructed as described by Pan et al. (2016). The
561 target sequence (TTGGAAAGGCAGTGAGATCA) was designed using a web tool of
562 CRISPR-P (Lei et al., 2014). The synthesized sequences were annealed and inserted into
563 *Bbs*I site of AtU6-sgRNA-AtUBQ-Cas9 vector, and the AtU6-sgRNA-AtUBQ-Cas9
564 cassette was inserted into the *Hind*III and *Kpn*I sites of pCAMBIA1301 binary vector. To
565 obtain the tomato *PGR5* overexpressing construct, the 357 bp full-length coding DNA
566 sequence (CDS) was amplified with the primers *PGR5*-OE-F and *PGR5*-OE-R
567 (Supplemental Table S3) using tomato cDNA as the template. The PCR product was
568 digested with *Asc*I and *Kpn*I and inserted behind the CaMV 35S promoter in the plant
569 transformation vector pFGC1008-HA. The resulting plasmids (*HY5*-OE-HA, *PGR5*
570 CRISPR/Cas9 vector and *PGR5*-OE-HA) were transformed into *Agrobacterium tumefaciens*
571 strain EHA105, and then introduced into tomato seeds of Ailsa Craig via a method as
572 previously described (Fillatti et al., 1987). Two independent homozygous lines of the F2
573 generation were used for the study. Two independent *pgr5* lines, *pgr5#4* and *pgr5#5* which
574 mutated at the first base of the protospacer adjacent motif (PAM) and stopped translation
575 immediately (Supplemental Fig. S10, A-C).
576 Seedlings were grown in pots with a mixture of three parts peat to one part vermiculite,
577 receiving Hoagland nutrient solution. The growth conditions were as follows: 12 h
578 photoperiod, temperature of 25/20 ^{o}C (day/night), and photosynthetic photo flux density
579 (PPFD) of 600 µmol m^{-2} s^{-1}.
580
581 **Cold, Light and Chemical Treatments**
582 Plants at the 11-leaf-stage were used for the determination of spatial variation in
583 photoinhibition. Experiments were carried out in growth rooms with a 12 h photoperiod, and
584 a PPFD of 200 µmol m^{-2} s^{-1} by providing white light from directly above the plants. Light
585 quality analysis revealed that R/FR ratios decreased from 1.3 at the 9th leaf rank to 0.5 at 5th
586 leaf rank. Growth room temperatures were controlled at either 25 ^{o}C (optimal growth
587 temperatures) or 4 ^{o}C (cold stress). Other light quality treatments were carried out in

588 controlled environment growth chambers (Conviron E15; Conviron, Manitoba, Canada) on
589 plants at the 6-leaf stage. Plants were grown under a 12/12 h light/dark cycle, with 85%
590 humidity. For these light quality treatments, plants were exposed to cold stress at 4 ^{o}C under
591 either high R/FR ratio (1.5), i.e. low FR intensity (L-FR, 133 µmol m^{-2} s^{-1}) or low R/FR
592 ratio (0.5), i.e. high FR intensity (H-FR, 400 µmol m^{-2} s^{-1}) light conditions. R light, supplied
593 by LED (λ_{max} = 660 nm, Philips, Netherland), was maintained at 200 µmol m^{-2} s^{-1}. FR was
594 supplied by a FR LED (λ_{max} = 735 nm, Philips, Netherland). R/FR ratios were calculated via
595 the quantum flux densities measured between 655 and 665 nm divided by the quantum flux
596 densities measured between 730 and 740 nm.
597 To determine the cause of light-induced changes in photooxidizable P700 in plants
598 exposed to low growth temperatures, fully expanded leaves were excised from the plants at
599 6-leaf stage and put onto petri dishes containing either water or 25 µM methyl viologen
600 (MV). Leaves were allowed to float on either 100 mL of 25 µM MV or water for 3 h in
601 darkness at 25 °C. The petri dishes were then transferred to the 4 °C chambers and exposed
602 to different light quality (L-FR or H-FR) conditions (R/FR ratio, 1.5 or 0.5) for 6 h. The
603 maximum level of P700 photooxidation ($\Delta P700_{max}$) was then determined in the MV-treated
604 leaves and water-treated controls using the Dual-PAM-100 system (Heinz Walz, Effeltrich,
605 Germany).
606
607 **Cold Tolerance Assays**
608 Cellular membrane permeability, measured as relative electrolyte leakage (REL), was
609 determined after 7 d exposure to the cold stress, as described previously (Cao et al., 2007).
610 Levels of oxidized leaf proteins were assayed by immunoblot detection as described
611 previously (Wang et al., 2016). Plant death was recorded after 6 days recovery from the cold
612 treatment, i.e. after return to optimal temperatures (25 ^{o}C) with a 12/12 h light/dark cycle
613 (PPFD of 600 µmol m^{-2} s^{-1}) and 85% humidity.
614
615 **Chlorophyll Fluorescence Measurements**
616 Plants were dark-adapted for 30 min prior to measurement. The maximum quantum
617 yield of PSII (*Fv/Fm*) and NPQ were determined with the Imaging-PAM (IMAG-MAXI;

618 Heinz Walz, Effeltrich, Germany) as previously described (Jin et al., 2014). qE was
619 simultaneously measured with the Dual-PAM-100 system (Heinz Walz, Effeltrich,
620 Germany). Fluorescence quenching was induced by 10 min of actinic illumination with
621 white light. The maximal fluorescence in the dark-adapted state (*Fm*) and in the light-
622 adapted state (*Fm′*) and after 10 min of dark relaxation following actinic illumination (*Fm″*)
623 were determined using a saturating pulse of light applied at 2 min intervals. Energy-
624 dependent quenching (qE) was calculated according to the equations qE = *Fm*/*Fm′* –
625 *Fm*/*Fm″* (Liu and Last, 2015).

626 P700 were measured simultaneously with the Dual-PAM-100 system (Heinz Walz,
627 Effeltrich, Germany) after leaves had dark-adapted for 30 min (to obtain open reaction
628 centers). The maximum P700 photooxidation level ($\Delta P700_{max}$) was determined using a
629 saturation pulse (100 ms; 10,000 μmol m^{-2} s^{-1}) under an FR background (720 nm; about 0.3
630 μmol m^{-2} s^{-1}) according to the method of Klughammer and Schreiber (2008). The decrease
631 in $\Delta P700_{max}$ is an indicator of PSI photoinhibition.

632 Post-illumination chlorophyll fluorescence (CEF around PSI) was monitored by the
633 transient increase of dark-level chlorophyll fluorescence after actinic light (AL) illumination
634 (250 μmol m^{-2} s^{-1} for 3 min) had been turned off by using a Dual-PAM-100 instrument
635 (Heinz Walz, Effeltrich, Germany; Nashilevitz et al., 2010).

636

637 **Activity of Antioxidant Enzymes and Pigment Analysis**

638 Frozen leaf segments (0.3 g) were ground with 2 mL ice-cold buffer containing 50 mM
639 PBS (pH 7.8), 0.2 mM EDTA, 2 mM AsA, and 2% (w/v) polyvinylpolypyrrolidone. The
640 homogenates were centrifuged at 4 °C for 20 min at 12,000 *g*, and the resulting supernatants
641 were used for the determination of enzymatic activity. The protein concentration was
642 determined with bovine serum albumin as standard (Bradford, 1976). The activity of
643 superoxide dismutase (SOD), ascorbate peroxidase (APX), monodehydroascorbate
644 reductase (MDAR), dehydroascorbate reductase (DHAR) and glutathione reductase (GR)
645 was measured following the protocol used as previously described (Xia et al., 2009).

646 Total pigments were extracted as previously described (Xu et al., 2006). Xanthophyll
647 cycle pigments (V, violaxanthin; A, antheraxanthin; Z, zeaxanthin) were analysed using a

648 C30 column (YMC Inc., Wilmington, NC) equipped for HPLC (Waters, Watford,
649 Hertfordshire, United Kingdom) as described previously (Xu et al., 2006), with the
650 following modification to the elution program. Mobile phases A (90% methanol), and B
651 (tert-butyl methyl ether) were applied as follows: 92% A, 8% B, a linear gradient to 75% A
652 and 25% B by 30 min, and gradient changed to 30% A, 70% B by 35 min, held until 50 min,
653 then changed to 92% A and 8% B by 50.01 min, and then held to the end of analysis (60
654 min). The de-epoxidation state of the xanthophyll cycle pigments is defined as the
655 (A+Z)/(V+A+Z) ratio, where A, Z, and V are the concentrations of antheraxanthin,
656 zeaxanthin and violaxanthin, respectively.
657
658 **Determination of Stomatal Aperture and Visualization of Cellular H_2O_2 Accumulation**
659 Tomato stomatal apertures were measured as described previously (Xia et al., 2014) by
660 peeling off the abaxial epidermises with forceps and floating it on a buffer containing 30
661 mM KCl, 10 mM 2-(*N*-morpholino)-ethanesulfonic acid (MES, pH 6.15). All images were
662 captured using a light microscope equipped with a digital camera (Leica Microsystems,
663 Wetzlar, Germany).
664 The localisation of H_2O_2 accumulation in leaves was visualised at the subcellular level
665 using cytochemical $CeCl_3$ staining and transmission electron microscopy (H7650, Hitachi,
666 Tokyo, Japan) as described previously (Xia et al, 2009).
667
668 **Thylakoid Isolation and Immunoblot Analysis**
669 Total protein was extracted from tomato leaves following exposure to a cold stress at 4
670 ^{o}C under either H-FR or L-FR light conditions for 1 d as described by Wang et al. (2016).
671 After quantification of total protein concentrations, samples of 50 µg protein were separated
672 by SDS-PAGE electrophoresis, and immuno-labelled with primary antibodies raised against
673 PsbS (AS09533; Agrisera, Sweden). Following incubation with secondary anti-rabbit
674 antibodies (Invitrogen, Sweden), enhanced chemical luminescence (ECL) was performed to
675 detect labelled proteins.
676 Fractions of intact chloroplasts were prepared from (10 g) leaves harvested from
677 tomato plants that had been grown at either 25 ^{o}C or 4 ^{o}C for 3 d under either H-FR or L-FR

678 conditions as described by Hertle et al. (2013). Thylakoid fractions were prepared from
679 isolated chloroplasts by osmotic rupture. After centrifugation (4 °C, 14,000 *g*, 3 min), the
680 pellet containing the thylakoid membranes was resuspended in a buffer containing 10 mM
681 Tris/HCl (pH 6.8), 10 mM $MgCl_2$ and 20 mM KCl. The chlorophyll (Chl) concentration of
682 the membranes was quantified spectrophotometrically as described by Porra et al. (1989).
683 The thylakoid membranes (15 µg Chl at 1 mg Chl/mL) were solubilized using 2% (wt/vol)
684 n-dodecyl-β-D-maltoside (β-DM; Anatrace), as described by Kromdijk et al. (2016).
685 Following incubation at 30 min at 4 °C with gentle agitation, insoluble fractions were
686 removed by centrifugation (15,000 *g*) for 10 min at 4°C. The solubilized membrane proteins
687 were subjected to SDS-PAGE (15% polyacrylamide) electrophoresis. Proteins were then
688 transferred on to nitrocellulose membranes (BioRad, Hercules, CA, USA), which were then
689 incubated with antibodies against PsaB (AS10695; Agrisera, Sweden) or PsaC (AS10939;
690 Agrisera, Sweden). Secondary antibodies use in these studies were anti-rabbit (Invitrogen,
691 Sweden). Signal detection was using enhanced chemical luminescence (ECL).

692 **RNA Extraction and qRT-PCR Analysis**

693 Total RNA was extracted from tomato leaves using RNAprep Pure Plant Kit (Tiangen
694 Biotech Co., Ltd. Beijing, China) according to the manufacturer's instruction. Residual
695 DNA was removed with RNase Mini Kit (Qiagen). The extracted RNA was reverse
696 transcribed using a ReverTra Ace qPCR RT Kit (Toyobo, Osaka, Japan), following the
697 manufacturer's recommendations. qRT-PCR experiments were performed using a Power
698 SYBR Green PCR Master Mix kit (Takara, Chiga, Japan). qRT-PCR was performed with 3
699 min at 95 °C, followed by 40 cycles of 30 s at 95 °C, 30 s at 58 °C and 1 min at 72 °C. The
700 tomato *ACTIN2* gene was used as an internal control. Primers sequence can be found in
701 Supplemental Table S4. The relative gene expression was calculated following previously
702 described formulae (Livak et al., 2001).
703

704 **RNA-seq Analysis**

705 For tomato RNA-seq analysis, leaves tissues from 6-leaf stage tomato seedlings were
706 collected from L-FR and H-FR treatments after 6 h under 4 °C to conduct the RNA-seq
707 analysis. Total RNA was isolated using TRIzol reagent (Biotopped) and RNA integrity was

708 evaluated using a Bioanalyzer 2100 (Agilent). The RNA samples were then subjected to
709 RNA sequencing by LC Sciences. Genes with P value < 0.05 and fold change ≥ 2 were
710 regarded as differentially expressed genes.
711
712 **Recombinant Protein and Electrophoretic Mobility Shift Assay**
713 The full-length coding region of HY5 was first PCR amplified using the primers in
714 Supplemental Table S3, then, the product was digested with *BamH*I and *Sac*I and ligated
715 into the same sites of pET-32a vector. The recombinant vector was transformed into *E. coli*
716 strain BL21 (DE3). The recombinant histidine-tagged HIS-HY5 proteins were induced by
717 isopropyl β-D-1-thiogalactopyranoside and purified following the instructions of the
718 Novagen pET purification system.
719 For binding assay, probes were biotin end-labeled following the instructions of the
720 Biotin 3' End DNA Labeling Kit (Pierce, 89818) and annealed to double-stranded probe
721 DNA by incubating sequentially at 95 ^{o}C for 5 min, then the temperature decreased from 95
722 ^{o}C to 55 ^{o}C by 40 cycles (-1 ^{o}C/cycle, 1 cycle/min), 55 ^{o}C for 30 min, from 55 ^{o}C to 25 ^{o}C
723 by 30 cycles (-1 ^{o}C/cycle, 1 cycle/min), finally, 4 ^{o}C for 5 min. EMSA of the HY5-DNA
724 complexes was performed using biotin-labeled probes according to the instructions of the
725 Light Shift Chemiluminescent EMSA kit (Thermo Fisher Scientific, 20148). Briefly, 0.5 μg
726 of HY5 fusion proteins were incubated together with biotin-labeled probes in 20 μL reaction
727 mixtures containing 10 mM Tris-HCl, 1 mM DTT, 150 mM KCl, 100 mM $ZnCl_2$, 50 ng μL^{-1}
728 poly (dI-dC), 2.5% glycerol, 0.05% Nonidet P-40, and 0.5 μg mL^{-1} BSA for 20 min at room
729 temperature and separated on 6% native polyacrylamide gels in Tris-glycine buffer at 100 V.
730 After electrophoresis, the gel was dried and autoradiographed as described previously (Xu et
731 al., 2014).
732
733 **Chromatin Immunoprecipitation (ChIP) Assay**
734 ChIP assays were performed following the instructions of the EpiQuik^{TM} Plant ChIP
735 Kit (Epigentek, P-2014) as described previously (Li et al., 2011). Approximately 1 g of leaf
736 tissue was harvested from *35S-HY5*-HA and wild-type plants after cold stress under H-FR
737 condition. Chromatin was immunoprecipitated with an anti-HA antibody (Pierce, 26183),

738 and the goat anti-mouse IgG (Millipore, AP124P) was used as the negative control. Both
739 immunoprecipitated DNA and input DNA were analyzed by qRT-PCR (Light Cycler;
740 Roche). Primers for ChIP-qPCR of the *ABI5* promoters were listed in Supplemental Table
741 S5. Each ChIP value was normalized to its respective input DNA value. All ChIP-qPCR
742 experiments were independently performed in triplicate.
743
744 **Statistical Analysis**
745 The experimental design was a completely randomized block design with four
746 replicates. Each replicate contained 6-12 plants. Analysis of variance (ANOVA) was used to
747 test for significance. When interaction terms were significant ($P < 0.05$), differences between
748 means were analyzed using Turkey comparisons. Significant differences between treatment
749 means are indicated by different letters.
750
751 Sequence data from this article can be found in the GenBank/EMBL data libraries
752 under the accession numbers listed in Supplemental Table S4.
753
754
755 **Figure Legends**
756 **Figure 1.** Spatial variation in photoinhibition is partially attributable to the changes in light
757 quality conditions. A and B, Maximum photochemical efficiency of PSII (Fv/Fm, A),
758 maximum P700 photooxidation level ($\Delta P700_{max}$, B) in leaves at the 9th (Up) and 5th (Down)
759 ranks from the base in plants at 11-leaf stage under white light conditions after exposure to
760 4 °C for 7 d. C and D, Fv/Fm (C) and $\Delta P700_{max}$ (D) at 4th leaves of the tomato plants at 6-
761 leaf stage grown in temperature-controlled chambers at 25 °C or 4 °C under L-FR or H-FR
762 light conditions for 7 d. The false color code depicted at the bottom of the image ranges
763 from 0 (black) to 1.0 (purple) represents the level of damage in leaves. E, Immunoblot
764 detection of thylakoid proteins (PsaB and PsaC) separated by SDS-PAGE. Detached leaves
765 were exposed to 25 ^{o}C or 4 ^{o}C for 3 d under L-FR or H-FR. F, Effect of methyl viologen
766 (MV) on the $\Delta P700_{max}$ under cold stress in different light quality. After treated with 25 μM
767 MV for 3 h in darkness at 25 °C, leaves were transferred to 4 °C for 6 h under different light

768 quality conditions. For the L-FR and H-FR, R/FR ratio at 1.5 and 0.5, respectively, plants
769 were kept at R conditions (200 µmol m^{-2} s^{-1}) supplemented with different intensities of FR
770 (133 and 400 µmol m^{-2} s^{-1}). Data are the means (±SD) of 4 biological replicates except for
771 Fv/Fm which was the mean for 15 leaves from independent plants. Different letters indicate
772 significant differences (P< 0.05) according to the Tukey's test.
773
774 **Figure 2.** Roles for tomato phytochromes in the light quality regulation of photoinhibition
775 and the expression of light signaling genes (*HY5* and *COP1*). A, Fv/Fm and $\Delta P700_{max}$ of the
776 tomato phytochrome mutant plants after exposure to a cold at 4 °C under L-FR or H-FR
777 light conditions for 7 d. B, Post-illumination chlorophyll fluorescence (CEF around PS I) in
778 tomato plants after exposure to a cold at 4 °C for 3 d under L-FR and H-FR conditions. C
779 and D, Changes of NPQ (C) and PsbS protein (D) in wild type (WT) and phytochrome
780 mutant plants exposed for either 3 d or 1 d to cold stress (at 4 °C) under L-FR and H-FR
781 light conditions. E, Levels of *HY5* and *COP1* transcripts at 6 h after tomato phytochrome
782 mutants were exposed to 4 °C under L-FR or H-FR light conditions. For the L-FR and H-FR,
783 R/FR ratio treatments of 1.5 or 0.5 respectively, plants were kept under R (200 µmol m^{-2} s^{-1})
784 light conditions, supplemented with different intensities of FR (133 and 400 µmol m^{-2} s^{-1}).
785 Data are the means (±SD) of 4 biological replicates except for Fv/Fm ratios, which are the
786 means of 15 leaves from independent plants. Different letters indicate significant differences
787 (P< 0.05) according to the Tukey's test.
788
789 **Figure 3.** HY5 alleviated photoinhibition by induction of photoprotection. A and B, Fv/Fm
790 (A) and $\Delta P700_{max}$ (B) of the wild type (WT), *HY5*-RNAi and *COP1*-RNAi tomato plants
791 after exposure to a cold stress at 4 °C under L-FR or H-FR light conditions for 7 d. The false
792 color code depicted at the bottom of the image ranges from 0 (black) to 1.0 (purple)
793 represents the level of damage in leaves. C and D, Post-illumination chlorophyll
794 fluorescence (CEF around PSI, C) and NPQ (D) in WT, *HY5*-RNAi and *COP1*-RNAi
795 tomato plants after exposure to 4 °C for 3 d under L-FR and H-FR conditions. E,
796 Immunoblot analysis of PsbS in WT, *HY5*-RNAi and *COP1*-RNAi tomato plants after
797 exposure to 4 °C for 1 d under L-FR and H-FR conditions. Samples were loaded at equal

798 total proteins amounts based on Coomassie blue. F, Activity of antioxidant enzymes (SOD,
799 APX, MDAR, DHAR and GR) involved in Foyer-Halliwell-Asada cycle after the WT, *HY5*-
800 RNAi and *COP1*-RNAi tomato plants exposure to 25 °C or 4 °C under L-FR or H-FR light
801 conditions for 3 d. For the L-FR and H-FR, R/FR ratio at 1.5 and 0.5, respectively, plants
802 were kept at R conditions (200 µmol m^{-2} s^{-1}) supplemented with different intensities of FR
803 (133 and 400 µmol m^{-2} s^{-1}). Data are the means (±SD) of 4 biological replicates except for
804 Fv/Fm ratios, which are the means of 15 leaves from independent plants. Different letters
805 indicate significant differences ($P < 0.05$) according to the Tukey's test.
806
807 **Figure 4.** HY5 induced transcript level of *ABI5* by binding to promoter of *ABI5*. A and B,
808 G-box elements in the promoter of tomato *ABI5* gene (A) and oligonucleotide used in the
809 electrophoretic mobility shift assays (EMSA, B). Numbering is from predicted
810 transcriptional start sites. The ABI5 probe contains one G-box (ABI5-G-wt), whereas in the
811 ABI5-G-mut1 and ABI5-G-mut2 probes the G-box core sequence was mutated. The WT
812 and mutated G-box sequences are underlined. The mutated bases were indicated in red. C,
813 HY5 directly binds to the G-box of *ABI5* promoter in vitro. Recombinant HY5 was purified
814 from *E. coli* cells and used for DNA binding assays with probes of ABI5-G-wt, ABI5-G-
815 mut1 and ABI5-G-mut2. The protein purified from empty vector was used as the negative
816 control. D, Direct binding of HY5 to the *ABI5* promoter was analyzed using ChIP-qPCR in
817 *35S-HY5-3HA*-overexpressing (*HY5*-OE#1) tomato plants. *HY5*-OE#1 plants at 6-leaf stage
818 were exposed to 4 ^{o}C under H-FR condition and input chromatin was isolated from leaf
819 samples at 6 h. The epitope-tagged HY5-chromatin complex was immunoprecipitated with
820 an anti-HA antibody. A control reaction was processed side-by-side using mouse IgG.
821 Input- and ChIP-DNA samples were quantified by qRT-PCR using primers specific for the
822 promoter of the *ABI5* gene. The ChIP results are presented as percentage of the input DNA.
823 OE, overexpressing; #1, line of *HY5*-OE plants. E and F, Transcript level of *ABI5* gene at 6
824 h after *HY5*-RNAi and *COP1*-RNAi tomato plants exposed to 25 °C or 4 °C under different
825 R/FR light regimes (E), and two independent *HY5* overexpressing transgenic tomato lines
826 (*HY5*-OE#1, OE#3) exposed to 4 °C under H-FR conditions (F). G, Transcript level of *ABI5*
827 gene at 6 h after WT and phytochromes mutants of tomato exposed to 4 °C under different

828 R/FR light regimes. For the L-FR and H-FR, R/FR ratio at 1.5 and 0.5, respectively, plants
829 were kept at R conditions (200 μmol m^{-2} s^{-1}) supplemented with different intensities of FR
830 (133 and 400 μmol m^{-2} s^{-1}). Four independent experiments were performed yielding similar
831 results. Different letters indicate significant differences (P< 0.05) according to the Tukey's
832 test.
833
834 **Figure 5.** Role of ABI5 in light quality-regulated photoinhibition and photoprotection. A
835 and B, Fv/Fm (A) and $\Delta P700_{max}$ (B) of the non-silenced (pTRV) and silenced (pTRV-*ABI5*)
836 tomato plants grown in temperature-controlled chambers at 25 °C or 4 °C under L-FR or H-
837 FR light conditions for 7 d. The false color code depicted at the bottom of the image ranges
838 from 0 (black) to 1.0 (purple) represents the level of damage in leaves. C and D, Post-
839 illumination chlorophyll fluorescence (CEF around PSI, C) and NPQ (D) in the pTRV and
840 pTRV-*ABI5* tomato plants after exposure to 4 °C for 3 d under L-FR and H-FR conditions.
841 E, Immunoblot analysis of PsbS in pTRV and pTRV-*ABI5* tomato plants after exposure to
842 4 °C for 1 d under L-FR and H-FR conditions. Samples were loaded at equal total proteins
843 amounts based on Coomassie blue. F, Activity of antioxidant enzymes (SOD, APX, MDAR,
844 DHAR and GR) involved in Foyer-Halliwell-Asada cycle after the pTRV and pTRV-*ABI5*
845 tomato plants exposure to 25 °C or 4 °C under L-FR or H-FR light conditions for 3 d. For
846 the L-FR and H-FR, R/FR ratio at 1.5 and 0.5, respectively, plants were kept at R conditions
847 (200 μmol m^{-2} s^{-1}) supplemented with different intensities of FR (133 and 400 μmol m^{-2} s^{-1}).
848 Data are the means (±SD) of 4 biological replicates except for Fv/Fm ratios, which are the
849 means of 15 leaves from independent plants. Different letters indicate significant differences
850 (P< 0.05) according to the Tukey's test.
851
852 **Figure 6**. *RBOH1*-dependent ROS production prevents plants from photoinhibition by
853 activating photoprotection. A and B, Transcript level of *RBOH1* gene at 6 h (A) and
854 cytochemical localization of H_2O_2 accumulation in leaf mesophyll cells at 1 d as visualized
855 by $CeCl_3$ staining and TEM (B) after pTRV and pTRV-*ABI5* tomato plants exposed to 4 °C
856 under different R/FR light regimes. The arrows indicate $CeCl_3$ precipitates. Scale
857 bars = 0.5 μm. C and D, Fv/Fm (C) and $\Delta P700_{max}$ (D) of the wild type (WT) and *RBOH1*-

858 RNAi tomato plants were exposed to 25 °C or 4 °C under L-FR or H-FR light conditions for
859 7 d. The false color code depicted at the bottom of the image ranges from 0 (black) to 1.0
860 (purple) represents the level of damage in leaves. E and F, Post-illumination chlorophyll
861 fluorescence (CEF around PSI, E) and NPQ (F) in the WT and *RBOH1*-RNAi tomato plants
862 after exposure to 4 °C for 3 d under L-FR and H-FR conditions. G, Immunoblot analysis of
863 PsbS in WT and *RBOH1*-RNAi tomato plants after exposure to 4 °C for 1 d under L-FR and
864 H-FR conditions. Samples were loaded at equal total proteins amounts based on Coomassie
865 blue. H, Activity of antioxidant enzymes (SOD, APX, MDAR, DHAR and GR) involved in
866 Foyer-Halliwell-Asada cycle after the WT and *RBOH1*-RNAi tomato plants exposure to
867 25 °C or 4 °C under L-FR or H-FR light conditions for 3 d. For the L-FR and H-FR, R/FR
868 ratio at 1.5 and 0.5, respectively, plants were kept at R conditions (200 µmol m^{-2} s^{-1})
869 supplemented with different intensities of FR (133 and 400 µmol m^{-2} s^{-1}). Data are the
870 means (±SD) of 4 biological replicates except for Fv/Fm ratios, which are the means of 15
871 leaves from independent plants. Different letters indicate significant differences (P< 0.05)
872 according to the Tukey's test.
873
874 **Figure 7**. *PROTON GRADIENT REGULATION5* (*PGR5*)-dependent CEF plays dual roles
875 in preventing plants from photoinhibition. A and B, Fv/Fm (A) and $\Delta P700_{max}$ (B) of the wild
876 type (WT), *pgr5* mutant (*pgr5#5*) and *PGR5*-overexpressing (OE-*PGR5#3*) transgenic
877 plants grown at 4 °C under L-FR or H-FR light conditions for 7 d. The false color code
878 depicted at the bottom of the image ranges from 0 (black) to 1.0 (purple) represents the level
879 of damage in leaves. C and D, qE (C) and NPQ (D) in the WT, *pgr5#5* mutant and OE-
880 *PGR5#3* tomato plants after exposure to 4 °C for 3 d under L-FR and H-FR conditions. E
881 and F, PsbS protein (E) and de-epoxidation state of the xanthophyll cycle (F) in the WT,
882 *pgr5*#5 mutant and OE-*PGR5#3* tomato plants after exposure to 4 °C for 1 d and 3 d,
883 respectively, under L-FR and H-FR conditions. For the L-FR and H-FR, R/FR ratio at 1.5
884 and 0.5, respectively, plants were kept at R conditions (200 µmol m^{-2} s^{-1}) supplemented with
885 different intensities of FR (133 and 400 µmol m^{-2} s^{-1}). Data are the means (±SD) of 4
886 biological replicates, except for Fv/Fm ratios, which are the means for 15 leaves from

887 independent plants. Different letters indicate significant differences ($P < 0.05$) according to
888 the Tukey's test.
889
890 **Supplemental Data**
891 The following supplemental materials are available.
892 **Supplemental Figure S1.** Effect of spatial variation on the cold tolerance of tomato.
893 **Supplemental Figure S2.** Effect of FR intensity on the cold tolerance and photoprotective
894 response of tomato.
895 **Supplemental Figure S3.** Silencing efficiency and cold tolerance of *HY5*-RNAi and *COP1*-
896 RNAi tomato plants.
897 **Supplemental Figure S4.** Cold tolerance of *HY5*-overexpressing transgenic tomato lines.
898 **Supplemental Figure S5.** Transcripts of genes involved in Foyer-Halliwell-Asada cycle in
899 WT, *HY5*-RNAi and *COP1*-RNAi tomato plants.
900 **Supplemental Figure S6.** HY5 regulated ABA-mediated stomatal movement and directly
901 binds to the G-boxes of the *ABI* promoters *in vitro*.
902 **Supplemental Figure S7.** Silencing efficiency and cold tolerance of *ABI5* silenced plants.
903 **Supplemental Figure S8.** Cold tolerance of WT and *RBOH1*-RNAi transgenic tomato
904 plants.
905 **Supplemental Figure S9.** Relative expression of CEF related genes in response to cold
906 stress and far red light.
907 **Supplemental Figure S10.** Transgenic tomato of *pgr5* mutant and *PGR5*-overexpressing
908 plants.
909 **Supplemental Figure S11.** Cold tolerance and cyclic electron flux (CEF) around PSI in
910 *pgr5* mutant and OE-*PGR5* plants.
911 **Supplemental Figure S12.** Changes of $\Delta P700_{max}$ in WT and OE-*PGR5* tomato plants as
912 altered by the silencing of *HY5*, *ABI5* or *RBOH1*.
913 **Supplemental Table S1.** Differentially expressed genes of tomato plants after exposure to a
914 cold at 4 °C under H-FR and L-FR light conditions.

915 **Supplemental Table S2.** Differentially expressed genes in the photosystems and
916 photoprotection of tomato plants after exposure to a cold at 4 °C under H-FR and L-FR light
917 conditions.
918 **Supplemental Table S3.** PCR primer sequences used for vector construction.
919 **Supplemental Table S4.** List of primer sequences used for qRT-PCR analysis.
920 **Supplemental Table S5.** Primers used for ChIP-qPCR assays.
921
922
923 **LITERATURE CITED**

924 **Ahn TK, Avenson TJ, Ballottari M, Cheng Y-C, Niyogi KK, Bassi R, Fleming GR**
925 (2008) Architecture of a charge-transfer state regulating light harvesting in a plant
926 antenna protein. Science **320**: 794-797
927 **Allorent G, Lefebvre-Legendre L, Chappuis R, Kuntz M, Truong TB, Niyogi KK, Ulm**
928 **R, Goldschmidt-Clermont M** (2016) UV-B photoreceptor-mediated protection of the
929 photosynthetic machinery in *Chlamydomonas reinhardtii*. Proc Natl Acad Sci USA
930 **113**: 14864-14869
931 **Allorent G, Petroutsos D** (2017) Photoreceptor-dependent regulation of photoprotection.
932 Curr Opin Plant Biol **37**: 102-108
933 **Ballaré CL** (2014) Light regulation of plant defense. Annu Rev Plant Biol **65:** 335-363
934 **Bradford MM** (1976) A rapid and sensitive method for the quantitation of microgram
935 quantities of protein utilizing the principle of protein-dye binding. Anal Biochem **72:**
936 248-254
937 **Cao WH, Liu J, He XJ, Mu RL, Zhou HL, Chen SY, Zhang JS** (2007) Modulation of
938 ethylene responses affects plant salt-stress responses. Plant Physiol **143:** 707-719
939 **Catala R, Medina J, Salinas J** (2011) Integration of low temperature and light signaling
940 during cold acclimation response in Arabidopsis. Proc Natl Acad Sci USA **108:** 16475-
941 16480
942 **Cerrudo I**, **Keller MM**, **Cargnel MD**, **Demkura PV**, **de Wit M**, **Patitucci MS, Pierik R,**
943 **Pieterse CMJ, Ballaré CL** (2012) Low red/far-red ratios reduce Arabidopsis

944 resistance to *Botrytis cinerea* and jasmonate responses via a COI1-JAZ10-dependent,
945 salicylic acid-independent mechanism. Plant Physiol **158:** 2042-2052
946 **Chen H, Zhang J, Neff MM, Hong SW, Zhang H, Deng XW, Xiong L** (2008) Integration
947 of light and abscisic acid signaling during seed germination and early seedling
948 development. Proc Natl Acad Sci USA **105:** 4495-4500
949 **Chen M, Chory J, Fankhauser C** (2004) Light signal transduction in higher plants. Annu
950 Rev Genet **38:** 87-117
951 **Chen Z, Gallie DR** (2012) Violaxanthin de-epoxidase is rate-limiting for non-
952 photochemical quenching under subsaturating light or during chilling in Arabidopsis.
953 Plant Physiol Biochem **58:** 66-82
954 **Cluis CP, Mouchel CF, Hardtke CS** (2004) The Arabidopsis transcription factor HY5
955 integrates light and hormone signaling pathways. Plant J **38:** 332-347
956 **Duan M, Ma NN, Li D, Deng YS, Kong FY, Lv W, Meng QW** (2012) Antisense-
957 mediated suppression of tomato thylakoidal ascorbate peroxidase influences
958 antioxidant network during chilling stress. Plant Physiol Biochem **58:** 37-45
959 **Fillatti JJ, Kiser J, Rose R, Comai L** (1987) Efficient transfer of a glyphosate tolerance
960 gene into tomato using a binary *Agrobacterium tumefaciens* vector. Bio-Technol **5:**
961 726-730
962 **Foyer CH, Neukermans J, Queval G, Noctor G, Harbinson J** (2012) Photosynthetic
963 control of electron transport and the regulation of gene expression. J Exp Bot **63:** 1637-
964 1661
965 **Foyer CH, Ruban AV, Noctor G** (2017) Viewing oxidative stress through the lens of
966 oxidative signalling rather than damage. Biochem J **474:** 877-883
967 **Foyer CH, Souriau N, Perret S, Lelandais M, Kunert KJ, Pruvost C, Jouanin L** (1995)
968 Overexpression of glutathione reductase but not glutathione synthetase leads to
969 increases in antioxidant capacity and resistance to photoinhibition in poplar trees. Plant
970 Physiol **109:** 1047-1057
971 **Franklin KA, Quail PH** (2010) Phytochrome functions in Arabidopsis development. J Exp
972 Bot **61:** 11-24

973 **Gangappa SN, Botto JF** (2016) The multifaceted roles of HY5 in plant growth and
974 development. Mol Plant **9:** 1353-1365
975 **Guo ZX, Wang F, Xiang X, Ahammed GJ, Wang MM, Onac E, Zhou J, Xia XJ, Shi K,**
976 **Yin XR, et al** (2016) Systemic induction of photosynthesis via illumination of the
977 shoot apex is mediated by phytochrome B. Plant Physiol **172:** 1259-1272
978 **Han H, Gao S, Li B, Dong XC, Feng HL, Meng QW** (2010) Overexpression of
979 violaxanthin de-epoxidase gene alleviates photoinhibition of PSII and PSI in tomato
980 during high light and chilling stress. J Plant Physiol **167:** 176-183
981 **Hertle AP, Blunder T, Wunder T, Pesaresi P, Pribil M, Armbruster U, Leister D** (2013)
982 PGRL1 is the elusive ferredoxin-plastoquinone reductase in photosynthetic cyclic
983 electron flow. Mol Cell **49:** 511-523
984 **Jiao Y, Lau OS, Deng XW** (2007) Light-regulated transcriptional networks in higher plants.
985 Nat Rev Genet **8:** 217-230
986 **Jin H, Liu B, Luo L, Feng D, Wang P, Liu J, Da Q, He Y, Qi K, Wang J, et al** (2014)
987 HYPERSENSITIVE TO HIGH LIGHT1 interacts with LOW QUANTUM YIELD OF
988 PHOTOSYSTEM II1 and functions in protection of photosystem II from photodamage
989 in Arabidopsis. Plant Cell **26:** 1213-1229
990 **Kasahara M, Kagawa T, Oikawa K, Suetsugu N, Miyao M, Wada M** (2002) Chloroplast
991 avoidance movement reduces photodamage in plants. Nature **420**: 829-832
992 **Kim HE, Tokura H** (1995) Influence of different light intensities during the daytime on
993 evening dressing behavior in the cold. Physiol Behav **58:** 779-783
994 **Kingston-Smith AH, Foyer CH** (2000) Bundle sheath proteins are more sensitive to
995 oxidative damage than those of the mesophyll in maize leaves exposed to paraquat or
996 low temperatures. J Expt Bot **51:** 123-130
997 **Kingston-Smith AH, Harbinson J, Williams J, Foyer CH** (1997) Effect of chilling on
998 carbon assimilation, enzyme activation, and photosynthetic electron transport in the
999 absence of photoinhibition in maize leaves. Plant Physiol **114:** 1039-1046
1000 **Klughammer C, Schreiber U** (2008) Saturation pulse method for assessment of energy
1001 conversion in PSI. PAM Application Notes **1:** 11-14

1002 **Kromdijk J, Głowacka K, Leonelli L, Gabilly ST, Iwai M, Niyogi KK, Long SP** (2016)
1003 Improving photosynthesis and crop productivity by accelerating recovery from
1004 photoprotection. Science **354:** 857-861
1005 **Lau OS, Deng XW** (2010) Plant hormone signaling lightens up: integrators of light and
1006 hormones. Curr Opin Plant Biol **13:** 571-577
1007 **Lei Y, Lu L, Liu HY, Li S, Xing F, Chen LL** (2014) CRISPR-P: A web tool for synthetic
1008 single-guide RNA design of CRISPR-system in plants. Mol Plant **7:** 1494-1496
1009 **Li XP, Mullermoule P, Gilmore AM, Niyogi KK** (2002) PsbS-dependent enhancement of
1010 feedback de-excitation protects photosystem II from photoinhibition. Proc Natl Acad
1011 Sci USA **99:** 15222-15227
1012 **Li ZF, Zhang LX, Yu YW, Quan RD, Zhang ZJ, Zhang HW, Huang RF** (2011) The
1013 ethylene response factor AtERF11 that is transcriptionally modulated by the bZIP
1014 transcription factor HY5 is a crucial repressor for ethylene biosynthesis in Arabidopsis.
1015 Plant J **68:** 88-99
1016 **Liu J, Last RL** (2015) A land plant-specific thylakoid membrane protein contributes to
1017 photosystem II maintenance in *Arabidopsis thaliana*. Plant J **82:** 731-743
1018 **Liu Y, Roof S, Ye Z, Barry C, van Tuinen A, Vrebalov J, Bowler C, Giovannoni J**
1019 (2004) Manipulation of light signal transduction as a means of modifying fruit
1020 nutritional quality in tomato. Proc Natl Acad Sci USA **101:** 9897-9902
1021 **Liu YL, Schiff M, Dinesh-Kumar SP** (2002) Virus-induced gene silencing in tomato.
1022 Plant J **31:**777-786
1023 **Livak KJ, Schmittgen TD** (2001) Analysis of relative gene expression data using real-time
1024 quantitative PCR and the $2^{-\Delta\Delta\Delta CT}$method. Methods **25:** 402-408
1025 **Maruta T, Tanouchi A, Tamoi M, Yabuta Y, Yoshimura K, Ishikawa T, Shigeoka S**
1026 (2010) Arabidopsis chloroplastic ascorbate peroxidase isoenzymes play a dual role in
1027 photoprotection and gene regulation under photooxidative stress. Plant Cell Physiol **51:**
1028 190-200
1029 **Mittal A, Gampala SSL, Ritchie GL, Payton P, Burke JJ, Rock CD** (2014) Related to
1030 ABA-insensitive 3 (ABI3)/Viviparous 1 and AtABI5 transcription factor coexpression
1031 in cotton enhances drought stress adaptation. Plant Biotechnol J **12:** 578-589

1032 **Möglich A, Yang X, Ayers RA, Moffat K** (2010) Structure and function of plant
1033 photoreceptors. Annu Rev Plant Biol **61:** 21-47
1034 **Munekage Y, Hashimoto M, Miyake C, Tomizawa KI, Endo T, Tasaka M, Shikanai T**
1035 (2004) Cyclic electron flow around photosystem I is essential for photosynthesis.
1036 Nature **429:** 579-582
1037 **Munekage Y, Hojo M, Meurer J, Endo T, Tasaka M, Shikanai T** (2002) PGR5 is
1038 involved in cyclic electron flow around photosystem I and is essential for
1039 photoprotection in Arabidopsis. Cell **110:** 361-371
1040 **Murata Y, Pei ZM, Mori IC, Schroeder JI** (2001) Abscisic acid activation of plasma
1041 membrane Ca^{2+} channels in guard cells requires cytosolic NADPH and is differentially
1042 disrupted upstream and downstream of reactive oxygen species production in *abi1-1*
1043 and *abi2-1* protein phosphatase 2C mutants. Plant Cell **13:** 2513-2523
1044 **Nagata M, Yamamoto N, Shigeyama T, Terasawa Y, Anai T, Sakai T, Inada S, Arima**
1045 **S, Hashiguchi M, Akashi R, et al** (2015) Red/Far red light controls arbuscular
1046 mycorrhizal colonization via jasmonic acid and strigolactone signaling. Plant Cell
1047 Physiol **56:** 2100-2109
1048 **Nashilevitz S, Melamed-Bessudo C, Izkovich Y, Rogachev I, Osorio S, Itkin M, Adato**
1049 **A, Pankratov I, Hirschberg J, Fernie AR, et al** (2010) An orange ripening mutant
1050 links plastid NAD(P)H dehydrogenase complex activity to central and specialized
1051 metabolism during tomato fruit maturation. Plant Cell **22:** 1977-1997
1052 **Nishiyama Y, Allakhverdiev SI, Murata N** (2006) A new paradigm for the action of
1053 reactive oxygen species in the photoinhibition of photosystem II. Biochim Biophys
1054 Acta **1757:** 742-749
1055 **Niyogi KK, Björkman O, Grossman AR** (1997) The roles of specific xanthophylls
1056 in photoprotection. Proc Natl Acad Sci USA **94:** 14162-14167
1057 **Niyogi KK, Grossman AR, Björkman O** (1998) Arabidopsis mutants define a central role
1058 for the xanthophyll cycle in the regulation of photosynthetic energy conversion. Plant
1059 Cell **10:** 1121-1134

1060 **Okegawa Y, Kagawa Y, Kobayashi Y, Shikanai T** (2008) Characterization of factors
1061 affecting the activity of photosystem I cyclic electron transport in chloroplasts. Plant
1062 Cell Physiol **49:** 825-834
1063 **Osterlund MT, Hardtke CS, Wei N, Deng XW** (2000) Targeted destabilization of HY5
1064 during light-regulated development of Arabidopsis. Nature **405:** 462-466
1065 **Pan CT, Ye L, Qin L, Liu X, He YJ, Wang J, Chen LF, Lu G** (2016) CRISPR/Cas9-
1066 mediated efficient and heritable targeted mutagenesis in tomato plants in the first and
1067 later generations. Sci Rep **6:** 24765
1068 **Petroutsos D, Tokutsu R, Maruyama S, Flori S, Greiner A, Magneschi L, Cusant L,**
1069 **Kottke T, Mittag M, Hegemann P, et al** (2016) A blue-light photoreceptor mediates
1070 the feedback regulation of photosynthesis. Nature **537**:563-566
1071 **Porra RJ, Thompson WA, Kriedemann PE** (1989) Determination of accurate extinction
1072 coefficients and simultaneous equations for assaying chlorophylls a and b extracted
1073 with four different solvents: Verification of the concentration of chlorophyll standards
1074 by atomic absorption spectroscopy. Biochim Biophys Acta **975:** 384-394
1075 **Quail PH** (2002a) Phytochrome photosensory signalling networks. Nat Rev Mol Cell Biol **3:**
1076 85-93
1077 **Quail PH** (2002b) Photosensory perception and signalling in plant cells: new paradigms?
1078 Curr Opin Cell Biol **14:** 180-188
1079 **Ruban AV, Berera R, Ilioaia C, van Stokkum IHM, Kennis JTM, Pascal AA, van**
1080 **Amerongen H, Robert B, Horton P, van Grondelle R** (2007) Identification of a
1081 mechanism of photoprotective energy dissipation in higher plants. Nature **450**: 575-578
1082 **Sasidharan R, Chinnappa CC, Voesenek LACJ, Pierik R** (2009) A molecular basis for
1083 the physiological variation in shade avoidance responses. Plant Signal Behav **4:** 528-
1084 529
1085 **Shikanai T** (2007) Cyclic electron transport around photosystem I: genetic approaches.
1086 Annu Rev Plant Biol **58:** 199-217
1087 **Strand DD, Livingston AK, Satoh-Cruz M, Froehlich JE, Maurino VG, Kramer DM**
1088 (2015) Activation of cyclic electron flow by hydrogen peroxide in vivo. Proc Natl
1089 Acad Sci USA **112:** 5539-5544

1090 **Takahashi S, Badger MR** (2011) Photoprotection in plants: a new light on photosystem II
1091 damage. Trends Plant Sci **16:** 53-60
1092 **Takahashi S, Milward SE, Fan DY, Chow WS, Badger MR** (2009) How does cyclic
1093 electron flow alleviate photoinhibition in Arabidopsis? Plant Physiol **149:** 1560-1567
1094 **Wang F, Guo ZX, Li HZ, Wang MM, Onac E, Zhou J, Xia XJ, Shi K, Yu JQ, Zhou**
1095 **YH** (2016) Phytochrome A and B function antagonistically to regulate cold tolerance
1096 via abscisic acid-dependent jasmonate signaling. Plant Physiol **170:** 459-471
1097 **Xia XJ, Gao CJ, Song LX, Zhou YH, Shi K, Yu JQ** (2014) Role of H_2O_2 dynamics in
1098 brassinosteroid-induced stomatal closure and opening in *Solanum lycopersicum*. Plant
1099 Cell Environ **37:** 2036-2050
1100 **Xia XJ, Wang YJ, Zhou YH, Tao Y, Mao WH, Shi K, Asami T, Chen ZX, Yu JQ** (2009)
1101 Reactive oxygen species are involved in brassinosteroid-induced stress tolerance in
1102 cucumber. Plant Physiol **150:** 801-814
1103 **Xie XZ, Xue YJ, Zhou JJ, Zhang B, Chang H, Takano M** (2011) Phytochromes regulate
1104 SA and JA signaling pathways in rice and are required for developmentally controlled
1105 resistance to *Magnaporthe grisea*. Mol Plant **4:** 688-696
1106 **Xing Y, Jia W, Zhang J** (2008) AtMKK1 mediates ABA-induced *CAT1* expression and
1107 H_2O_2 production via AtMPK6-coupled signaling in Arabidopsis. Plant J **54:** 440-451
1108 **Xu CJ, Fraser PD, Wang WJ, Bramley PM** (2006) Differences in the carotenoid content
1109 of ordinary citrus and lycopene-accumulating mutants. J Agric Food Chem **54:** 5474-
1110 5481
1111 **Xu D, Li J, Gangappa SN, Hettiarachchi C, Lin F, Andersson MX, Jiang Y, Deng XW,**
1112 **Holm M** (2014) Convergence of light and ABA signaling on the ABI5 promoter. PLoS
1113 Genet **10:** e1004197
1114 **Yamori W, Makino A, Shikanai T** (2016) A physiological role of cyclic electron transport
1115 around photosystem I in sustaining photosynthesis under fluctuating light in rice. Sci
1116 Rep **6:** 20147
1117 **Yi C, Deng XW** (2005) COP1 from plant photomorphogenesis to mammalian
1118 tumorigenesis. Trends Cell Biol **15:** 618-625

1119 **de Wit M**, **Spoel SH**, **Sanchez-Perez GF**, **Gommers CMM**, **Pieterse CMJ**, **Voesenek**
1120 **LACJ, Pierik R** (2013) Perception of low red:far-red ratio compromises both salicylic
1121 acid- and jasmonic acid-dependent pathogen defences in Arabidopsis. Plant J **75:** 90-
1122 103
1123 **Zhang AY, Jiang MY, Zhang JH, Ding HD, Xu SC, Hu XL, Tan MP** (2007) Nitric oxide
1124 induced by hydrogen peroxide mediates abscisic acid-induced activation of the
1125 mitogen-activated protein kinase cascade involved in antioxidant defense in maize
1126 leaves. New Phytol **175:** 36-50
1127 **Zhao Y, Chan Z, Xing L, Liu XD, Hou YJ, Chinnusamy V, Wang P, Duan C, Zhu JK**
1128 (2013) The unique mode of action of a divergent member of the ABA-receptor protein
1129 family in ABA and stress signaling. Cell Res **23:** 1380-1395
1130 **Zhou J, Wang J, Li X, Xia XJ, Zhou YH, Shi K, Chen ZX, Yu JQ** (2014) H_2O_2 mediates
1131 the crosstalk of brassinosteroid and abscisic acid in tomato responses to heat and
1132 oxidative stresses. J Exp Bot **65:** 4371-4383
1133 **Zhou J, Wang J, Shi K, Xia XJ, Zhou YH, Yu JQ** (2012) Hydrogen peroxide is involved
1134 in the cold acclimation-induced chilling tolerance of tomato plants. Plant Physiol
1135 Biochem **60:** 141-149
1136 **Zhu J, Dong CH, Zhu JK** (2007) Interplay between cold-responsive gene regulation,
1137 metabolism and RNA processing during plant cold acclimation. Curr Opin Plant Biol
1138 **10:** 290-295
1139

1140

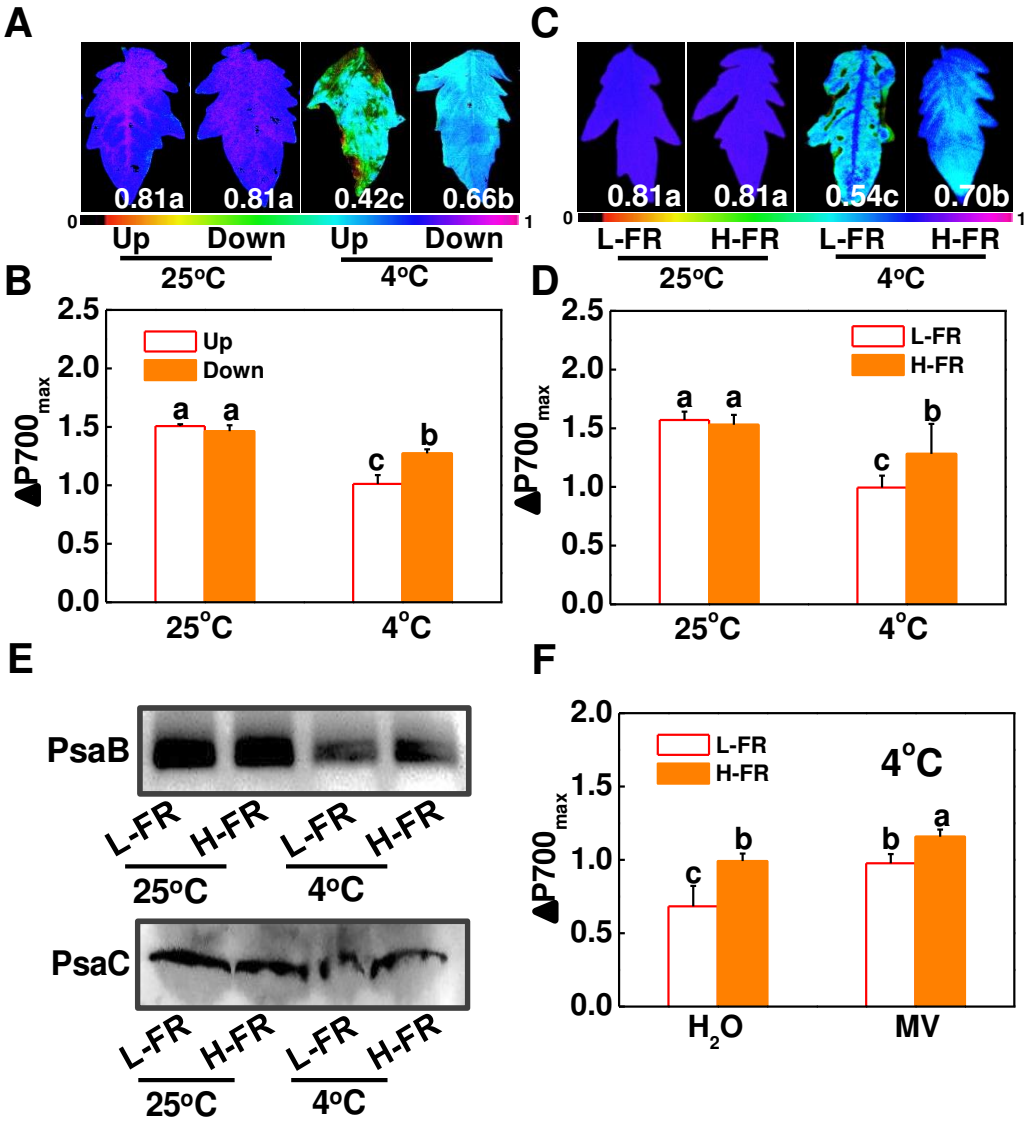

Figure 1. Spatial variation in photoinhibition is partially attributable to the changes in light quality conditions. A and B, Maximum photochemical efficiency of PSII (Fv/Fm, A), maximum P700 photooxidation level ($\Delta P700_{max}$, B) in leaves at the 9th (Up) and 5th (Down) ranks from the base in plants at 11-leaf stage under white light conditions after exposure to 4 °C for 7 d. C and D, Fv/Fm (C) and $\Delta P700_{max}$ (D) at 4th leaves of the tomato plants at 6-leaf stage grown in temperature-controlled chambers at 25 °C or 4 °C under L-FR or H-FR light conditions for 7 d. The false color code depicted at the bottom of the image ranges from 0 (black) to 1.0 (purple) represents the level of damage in leaves. E, Immunoblot detection of thylakoid proteins (PsaB and PsaC) separated by SDS-PAGE. Detached leaves were exposed to 25 °C or 4 °C for 3 d under L-FR or H-FR. F, Effect of methyl viologen (MV) on the $\Delta P700_{max}$ under cold stress in different light quality. After treated with 25 µM MV for 3 h in darkness at 25 °C, leaves were transferred to 4 °C for 6 h under different light quality conditions. For the L-FR and H-FR, R/FR ratio at 1.5 and 0.5, respectively, plants were kept at R conditions (200 µmol m^{-2} s^{-1}) supplemented with different intensities of FR (133 and 400 µmol m^{-2} s^{-1}). Data are the means (±SD) of 4 biological replicates except for Fv/Fm which was the mean for 15 leaves from independent plants. Different letters indicate significant differences (P< 0.05) according to the Tukey's test.

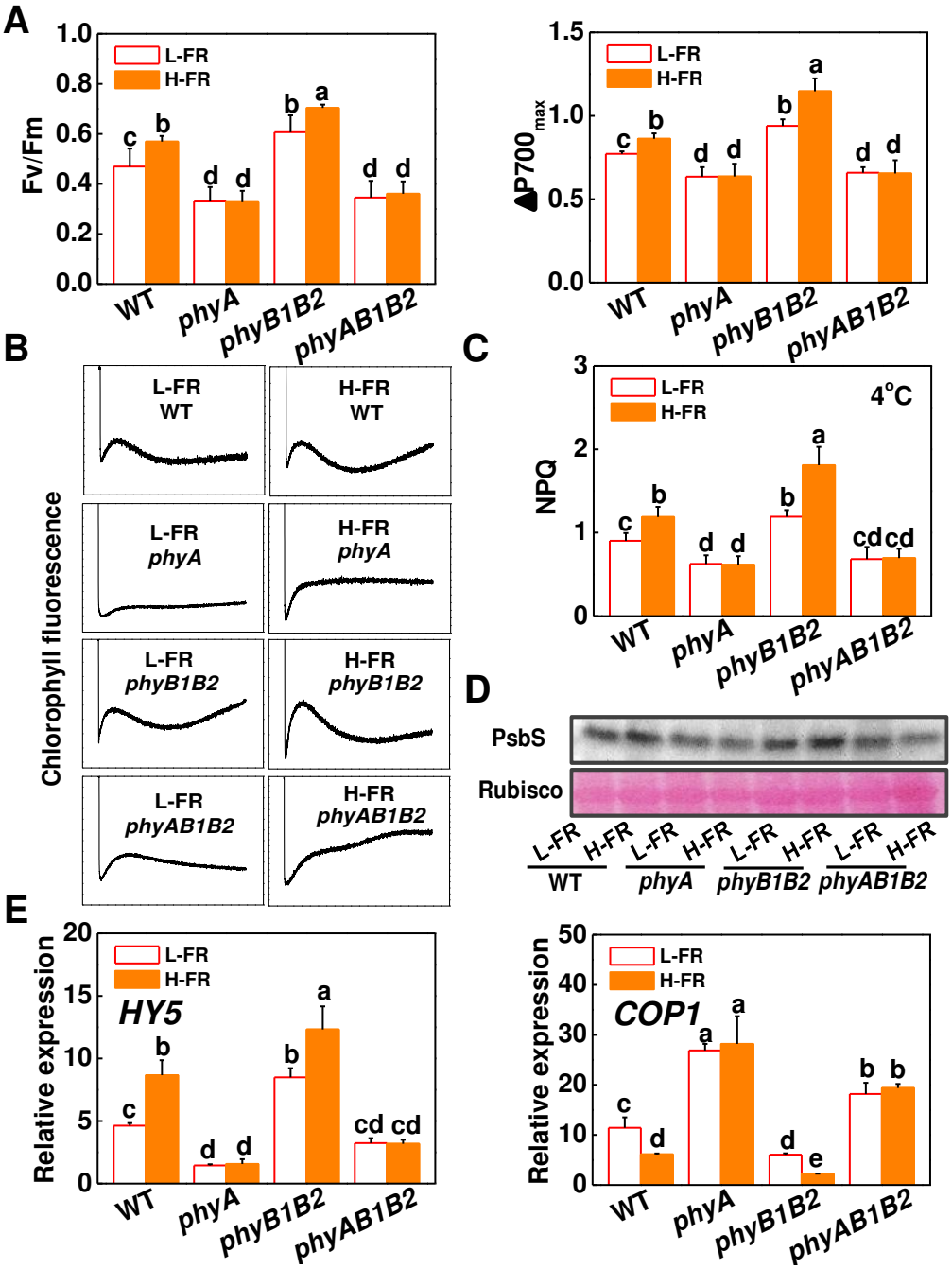

Figure 2. Roles for tomato phytochromes in the light quality regulation of photoinhibition and the expression of light signaling genes (HY5 and COP1). A, Fv/Fm and $\Delta P700_{max}$ of the tomato phytochrome mutant plants after exposure to a cold at 4 °C under L-FR or H-FR light conditions for 7 d. B, Post-illumination chlorophyll fluorescence (CEF around PS I) in tomato plants after exposure to a cold at 4 °C for 3 d under L-FR and H-FR conditions. C and D, Changes of NPQ (C) and PsbS protein (D) in wild type (WT) and phytochrome mutant plants exposed for either 3 d or 1 d to cold stress (at 4 °C) under L-FR and H-FR light conditions. E, Levels of HY5 and COP1 transcripts at 6 h after tomato phytochrome mutants were exposed to 4 °C under L-FR or H-FR light conditions. For the L-FR and H-FR, R/FR ratio treatments of 1.5 or 0.5 respectively, plants were kept under R (200 µmol m^{-2} s^{-1}) light conditions, supplemented with different intensities of FR (133 and 400 µmol m^{-2} s^{-1}). Data are the means (±SD) of 4 biological replicates except for Fv/Fm ratios, which are the means of 15 leaves from independent plants. Different letters indicate significant differences (P< 0.05) according to the Tukey's test.

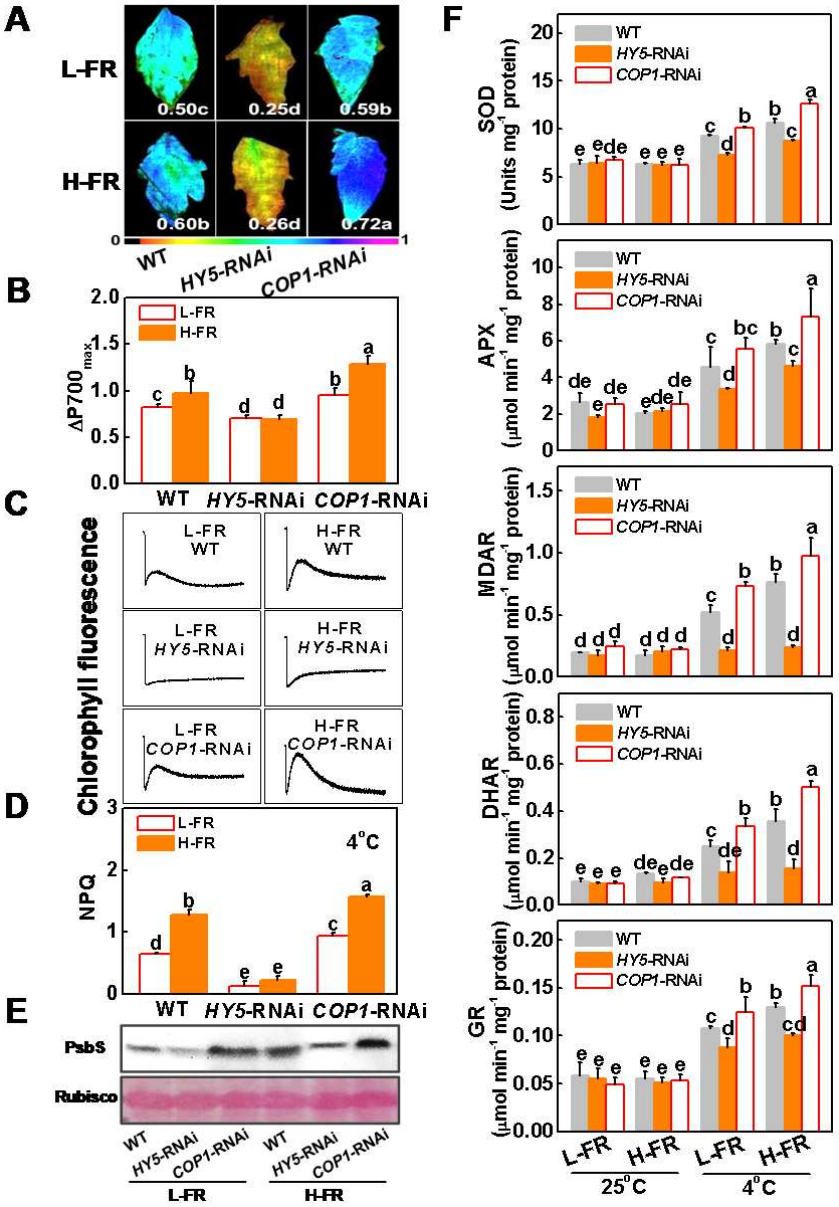

Figure 3. HY5 alleviated photoinhibition by induction of photoprotection. A and B, Fv/Fm (A) and $\Delta P700_{max}$ (B) of the wild type (WT), *HY5*-RNAi and *COP1*-RNAi tomato plants after exposure to a cold stress at 4 °C under L-FR or H-FR light conditions for 7 d. The false color code depicted at the bottom of the image ranges from 0 (black) to 1.0 (purple) represents the level of damage in leaves. C and D, Post-illumination chlorophyll fluorescence (CEF around PSI, C) and NPQ (D) in WT, *HY5*-RNAi and *COP1*-RNAi tomato plants after exposure to 4 °C for 3 d under L-FR and H-FR conditions. E, Immunoblot analysis of PsbS in WT, *HY5*-RNAi and *COP1*-RNAi tomato plants after exposure to 4 °C for 1 d under L-FR and H-FR conditions. Samples were loaded at equal total proteins amounts based on Coomassie blue. F, Activity of antioxidant enzymes (SOD, APX, MDAR, DHAR and GR) involved in Foyer-Halliwell-Asada cycle after the WT, *HY5*-RNAi and *COP1*-RNAi tomato plants exposure to 25 °C or 4 °C under L-FR or H-FR light conditions for 3 d. For the L-FR and H-FR, R/FR ratio at 1.5 and 0.5, respectively, plants were kept at R conditions (200 μmol m^{-2} s^{-1}) supplemented with different intensities of FR (133 and 400 μmol m^{-2} s^{-1}). Data are the means (±SD) of 4 biological replicates except for Fv/Fm ratios, which are the means of 15 leaves from independent plants. Different letters indicate significant differences (P< 0.05) according to the Tukey's test.

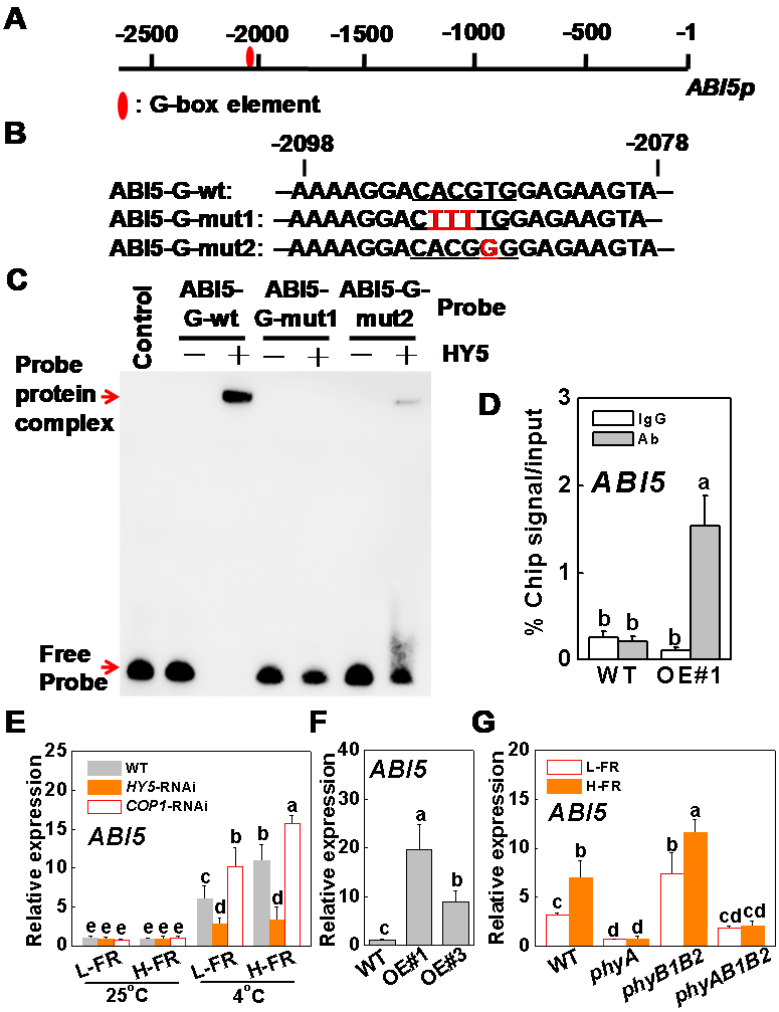

Figure 4. HY5 induced transcript level of *ABI5* by binding to promoter of *ABI5*. A and B, G-box elements in the promoter of tomato *ABI5* gene (A) and oligonucleotide used in the electrophoretic mobility shift assays (EMSA, B). Numbering is from predicted transcriptional start sites. The ABI5 probe contains one G-box (ABI5-G-wt), whereas in the ABI5-G-mut1 and ABI5-G-mut2 probes the G-box core sequence was mutated. The WT and mutated G-box sequences are underlined. The mutated bases were indicated in red. C, HY5 directly binds to the G-box of *ABI5* promoter in vitro. Recombinant HY5 was purified from *E. coli* cells and used for DNA binding assays with probes of ABI5-G-wt, ABI5-G-mut1 and ABI5-G-mut2. The protein purified from empty vector was used as the negative control. D, Direct binding of HY5 to the *ABI5* promoter was analyzed using ChIP-qPCR in *35S-HY5-3HA*-overexpressing (*HY5*-OE#1) tomato plants. *HY5*-OE#1 plants at 6-leaf stage were exposed to 4 ^{o}C under H-FR condition and input chromatin was isolated from leaf samples at 6 h. The epitope-tagged HY5-chromatin complex was immunoprecipitated with an anti-HA antibody. A control reaction was processed side-by-side using mouse IgG. Input- and ChIP-DNA samples were quantified by qRT-PCR using primers specific for the promoter of the *ABI5* gene. The ChIP results are presented as percentage of the input DNA. OE, overexpressing; #1, line of *HY5*-OE plants. E and F, Transcript level of *ABI5* gene at 6 h after *HY5*-RNAi and *COP1*-RNAi tomato plants exposed to 25 °C or 4 °C under different R/FR light regimes (E), and two independent *HY5* overexpressing transgenic tomato lines (*HY5*-OE#1, OE#3) exposed to 4 °C under H-FR conditions (F). G, Transcript level of *ABI5* gene at 6 h after WT and phytochromes mutants of tomato exposed to 4 °C under different R/FR light regimes. For the L-FR and H-FR, R/FR ratio at 1.5 and 0.5, respectively, plants were kept at R conditions (200 µmol m^{-2} s^{-1}) supplemented with different intensities of FR (133 and 400 µmol m^{-2} s^{-1}). Four independent experiments were performed yielding similar results. Different letters indicate significant differences (P< 0.05) according to the Tukey's test.

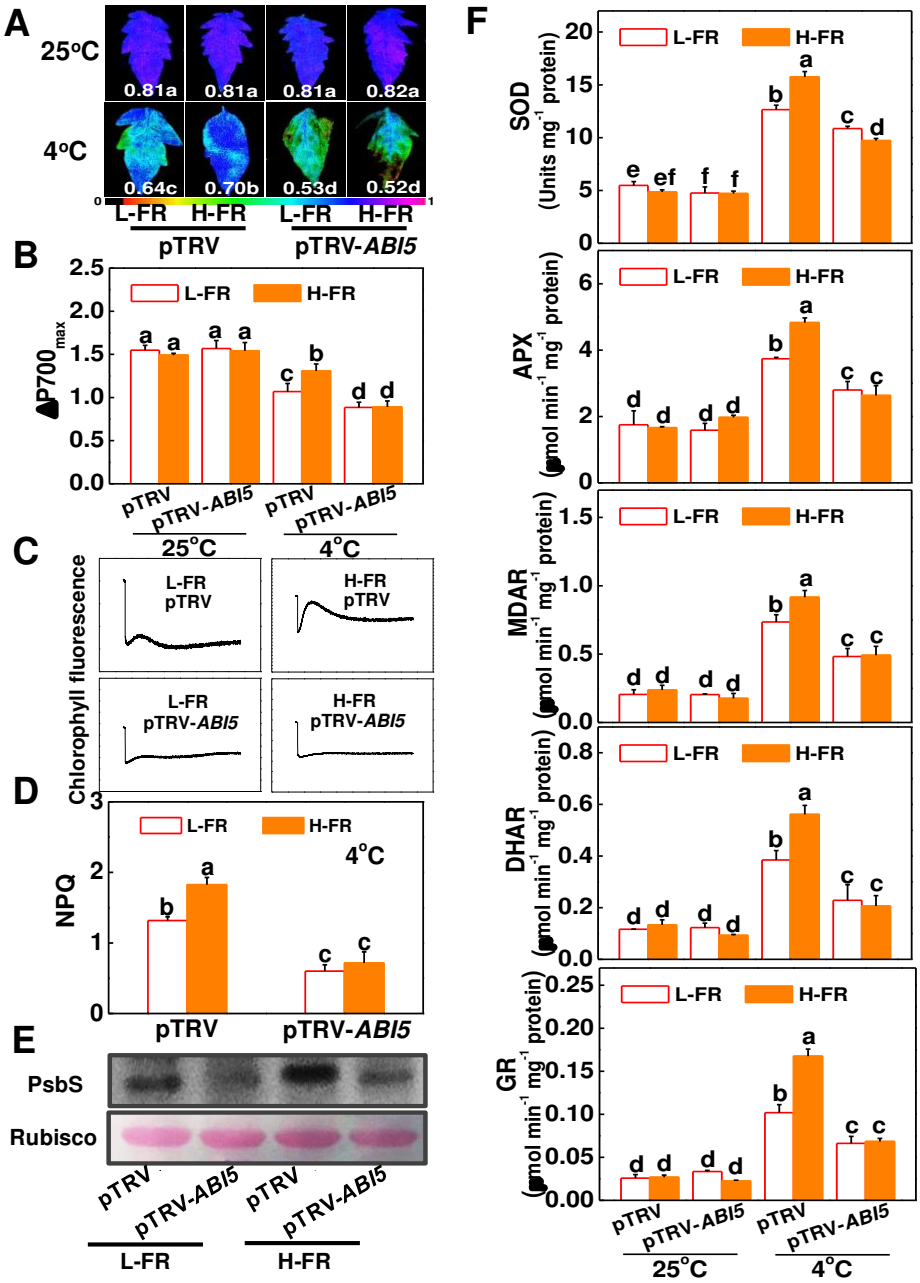

Figure 5. Role of *ABI5* in light quality-regulated photoinhibition and photoprotection. A and B, Fv/Fm (A) and $\Delta P700_{max}$ (B) of the non-silenced (pTRV) and silenced (pTRV-*ABI5*) tomato plants grown in temperature-controlled chambers at 25 °C or 4 °C under L-FR or H-FR light conditions for 7 d. The false color code depicted at the bottom of the image ranges from 0 (black) to 1.0 (purple) represents the level of damage in leaves. C and D, Post-illumination chlorophyll fluorescence (CEF around PSI, C) and NPQ (D) in the pTRV and pTRV-*ABI5* tomato plants after exposure to 4 °C for 3 d under L-FR and H-FR conditions. E, Immunoblot analysis of PsbS in pTRV and pTRV-*ABI5* tomato plants after exposure to 4 °C for 1 d under L-FR and H-FR conditions. Samples were loaded at equal total proteins amounts based on Coomassie blue. F, Activity of antioxidant enzymes (SOD, APX, MDAR, DHAR and GR) involved in Foyer-Halliwell-Asada cycle after the pTRV and pTRV-*ABI5* tomato plants exposure to 25 °C or 4 °C under L-FR or H-FR light conditions for 3 d. For the L-FR and H-FR, R/FR ratio at 1.5 and 0.5, respectively, plants were kept at R conditions (200 μmol m^{-2} s^{-1}) supplemented with different intensities of FR (133 and 400 μmol m^{-2} s^{-1}). Data are presented as the mean of 4 biological replicates (±SD) except for Fv/Fm which was the mean for 15 leaves from independent plants. Different letters indicate significant differences ($P < 0.05$) according to the Tukey's test.

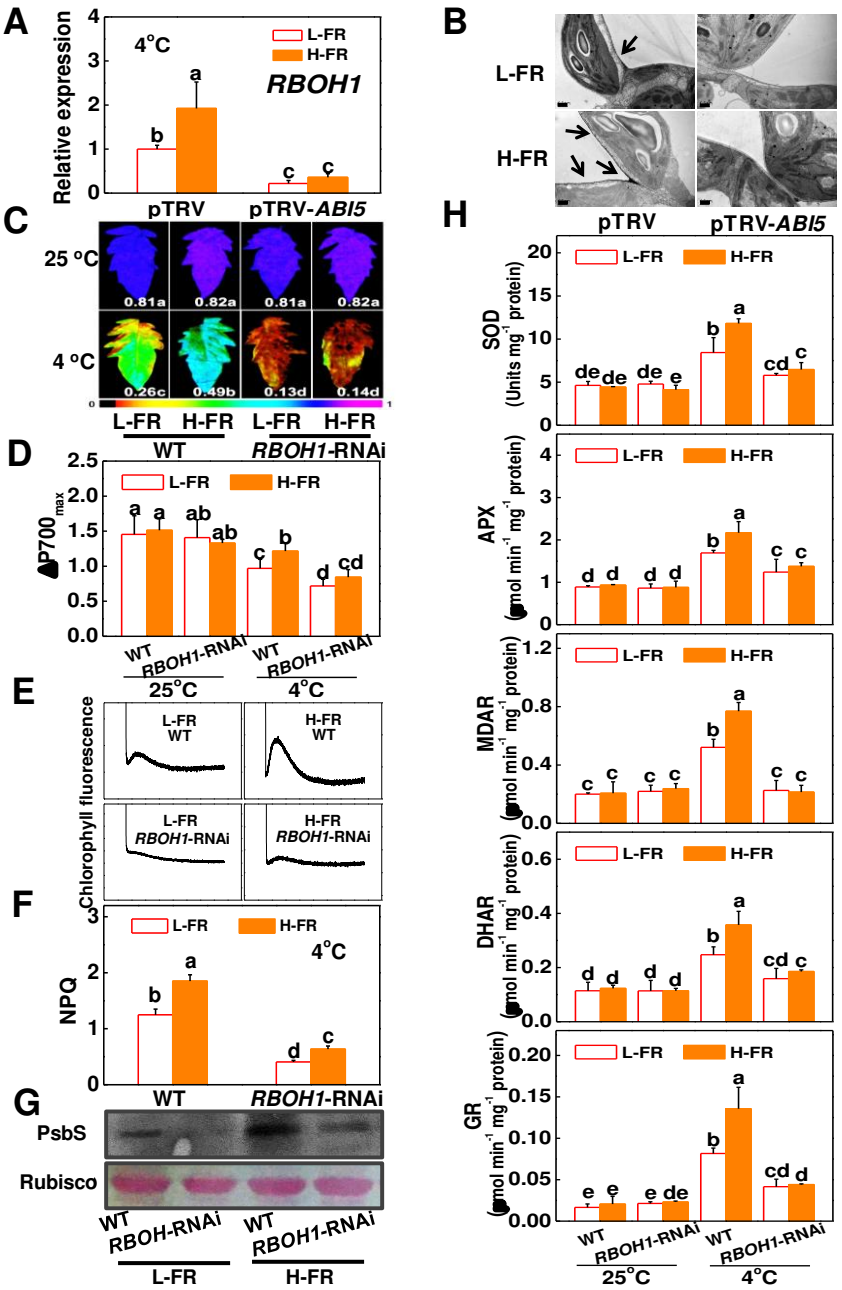

Figure 6. *RBOH1*-dependent ROS production prevents plants from photoinhibition by activating photoprotection. A and B, Transcript level of *RBOH1* gene at 6 h (A) and cytochemical localization of H_2O_2 accumulation in leaf mesophyll cells at 1 d as visualized by $CeCl_3$ staining and TEM (B) after pTRV and pTRV-*ABI5* tomato plants exposed to 4 °C under different R/FR light regimes. The arrows indicate $CeCl_3$ precipitates. Scale bars = 0.5 µm. C and D, Fv/Fm (C) and $\Delta P700_{max}$ (D) of the wild type (WT) and *RBOH1*-RNAi tomato plants were exposed to 25 °C or 4 °C under L-FR or H-FR light conditions for 7 d. The false color code depicted at the bottom of the image ranges from 0 (black) to 1.0 (purple) represents the level of damage in leaves. E and F, Post-illumination chlorophyll fluorescence (CEF around PSI, E) and NPQ (F) in the WT and *RBOH1*-RNAi tomato plants after exposure to 4 °C for 3 d under L-FR and H-FR conditions. G, Immunoblot analysis of PsbS in WT and *RBOH1*-RNAi tomato plants after exposure to 4 °C for 1 d under L-FR and H-FR conditions. Samples were loaded at equal total proteins amounts based on Coomassie blue. H, Activity of antioxidant enzymes (SOD, APX, MDAR, DHAR and GR) involved in Foyer-Halliwell-Asada cycle after the WT and *RBOH1*-RNAi tomato plants exposure to 25 °C or 4 °C under L-FR or H-FR light conditions for 3 d. For the L-FR and H-FR, R/FR ratio at 1.5 and 0.5, respectively, plants were kept at R conditions (200 µmol m^{-2} s^{-1}) supplemented with different intensities of FR (133 and 400 µmol m^{-2} s^{-1}). Data are the means (±SD) of 4 biological replicates except for Fv/Fm ratios, which are the means of 15 leaves from independent plants. Different letters indicate significant differences (P< 0.05) according to the Tukey's test.

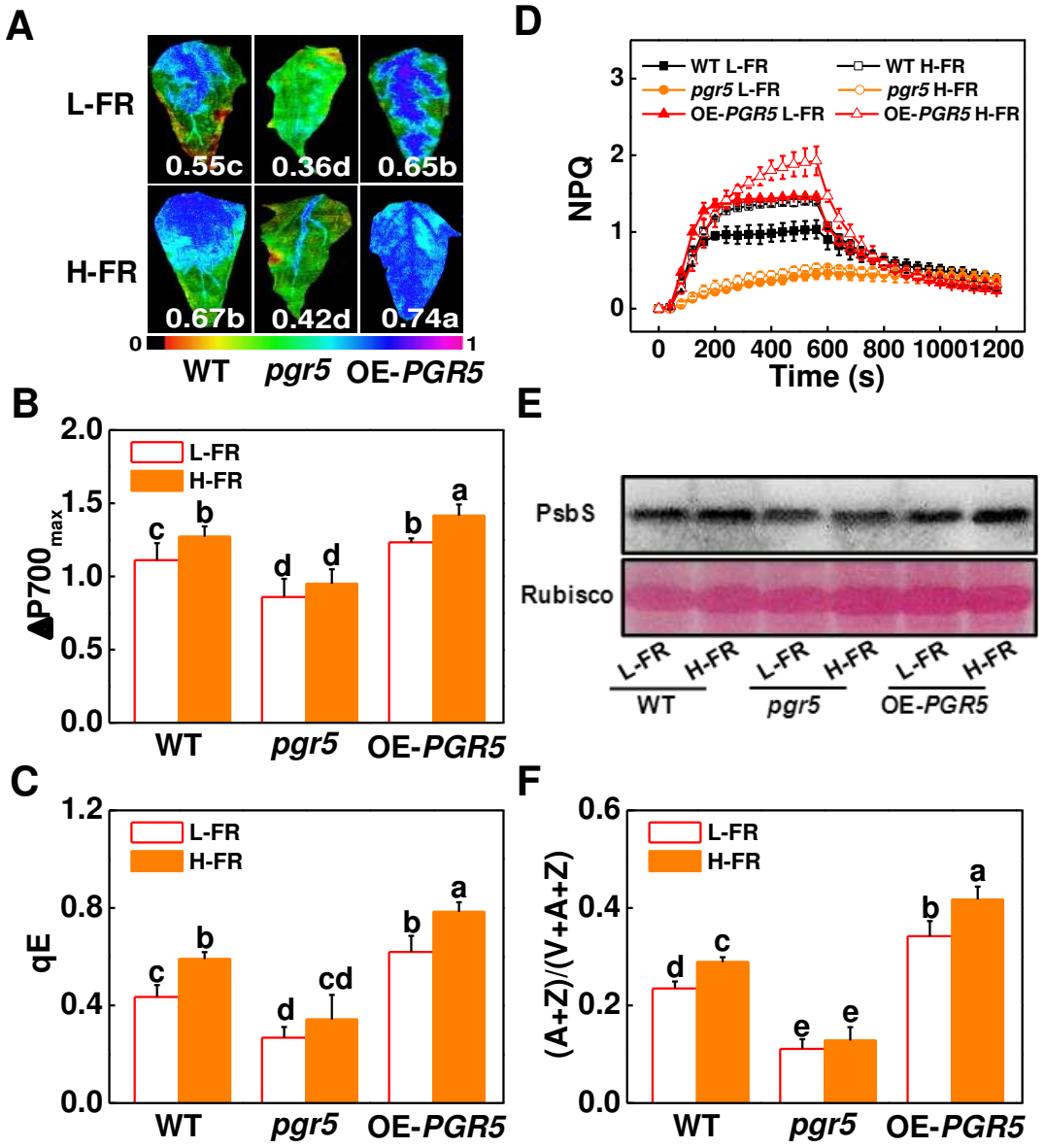

Figure 7. *PROTON GRADIENT REGULATION5* (*PGR5*)-dependent CEF plays dual roles in preventing plants from photoinhibition. A and B, Fv/Fm (A) and $\Delta P700_{max}$ (B) of the wild type (WT), *pgr5* mutant (*pgr5#5*) and *PGR5*-overexpressing (OE-*PGR5#3*) transgenic plants grown at 4 °C under L-FR or H-FR light conditions for 7 d. The false color code depicted at the bottom of the image ranges from 0 (black) to 1.0 (purple) represents the level of damage in leaves. C and D, qE (C) and NPQ (D) in the WT, *pgr5#5* mutant and OE-*PGR5#3* tomato plants after exposure to 4 °C for 3 d under L-FR and H-FR conditions. E and F, PsbS protein (E) and de-epoxidation state of the xanthophyll cycle (F) in the WT, *pgr5*#5 mutant and OE-*PGR5#3* tomato plants after exposure to 4 °C for 1 d and 3 d, respectively, under L-FR and H-FR conditions. For the L-FR and H-FR, R/FR ratio at 1.5 and 0.5, respectively, plants were kept at R conditions (200 µmol m^{-2} s^{-1}) supplemented with different intensities of FR (133 and 400 µmol m^{-2} s^{-1}). Data are the means (±SD) of 4 biological replicates, except for Fv/Fm ratios, which are the means for 15 leaves from independent plants. Different letters indicate significant differences (P< 0.05) according to the Tukey's test.

Parsed Citations

Ahn TK, Avenson TJ, Ballottari M, Cheng Y-C, Niyogi KK, Bassi R, Fleming GR (2008) Architecture of a charge-transfer state regulating light harvesting in a plant antenna protein. Science 320: 794-797
Pubmed: Author and Title
CrossRef: Author and Title
Google Scholar: Author Only Title Only Author and Title

Allorent G, Lefebvre-Legendre L, Chappuis R, Kuntz M, Truong TB, Niyogi KK, Ulm R, Goldschmidt-Clermont M (2016) UV-B photoreceptor-mediated protection of the photosynthetic machinery in Chlamydomonas reinhardtii. Proc Natl Acad Sci USA 113: 14864-14869
Pubmed: Author and Title
CrossRef: Author and Title
Google Scholar: Author Only Title Only Author and Title

Allorent G, Petroutsos D (2017) Photoreceptor-dependent regulation of photoprotection. Curr Opin Plant Biol 37: 102-108
Pubmed: Author and Title
CrossRef: Author and Title
Google Scholar: Author Only Title Only Author and Title

Ballaré CL (2014) Light regulation of plant defense. Annu Rev Plant Biol 65: 335-363
Pubmed: Author and Title
CrossRef: Author and Title
Google Scholar: Author Only Title Only Author and Title

Bradford MM (1976) A rapid and sensitive method for the quantitation of microgram quantities of protein utilizing the principle of protein-dye binding. Anal Biochem 72: 248-254
Pubmed: Author and Title
CrossRef: Author and Title
Google Scholar: Author Only Title Only Author and Title

Cao WH, Liu J, He XJ, Mu RL, Zhou HL, Chen SY, Zhang JS (2007) Modulation of ethylene responses affects plant salt-stress responses. Plant Physiol 143: 707-719
Pubmed: Author and Title
CrossRef: Author and Title
Google Scholar: Author Only Title Only Author and Title

Catala R, Medina J, Salinas J (2011) Integration of low temperature and light signaling during cold acclimation response in Arabidopsis. Proc Natl Acad Sci USA 108: 16475-16480
Pubmed: Author and Title
CrossRef: Author and Title
Google Scholar: Author Only Title Only Author and Title

Cerrudo I, Keller MM, Cargnel MD, Demkura PV, de Wit M, Patitucci MS, Pierik R, Pieterse CMJ, Ballaré CL (2012) Low red/far-red ratios reduce Arabidopsis resistance to Botrytis cinerea and jasmonate responses via a COI1-JAZ10-dependent, salicylic acid-independent mechanism. Plant Physiol 158: 2042-2052
Pubmed: Author and Title
CrossRef: Author and Title
Google Scholar: Author Only Title Only Author and Title

Chen H, Zhang J, Neff MM, Hong SW, Zhang H, Deng XW, Xiong L (2008) Integration of light and abscisic acid signaling during seed germination and early seedling development. Proc Natl Acad Sci USA 105: 4495-4500
Pubmed: Author and Title
CrossRef: Author and Title
Google Scholar: Author Only Title Only Author and Title

Chen M, Chory J, Fankhauser C (2004) Light signal transduction in higher plants. Annu Rev Genet 38: 87-117
Pubmed: Author and Title
CrossRef: Author and Title
Google Scholar: Author Only Title Only Author and Title

Chen Z, Gallie DR (2012) Violaxanthin de-epoxidase is rate-limiting for non-photochemical quenching under subsaturating light or during chilling in Arabidopsis. Plant Physiol Biochem 58: 66-82
Pubmed: Author and Title
CrossRef: Author and Title
Google Scholar: Author Only Title Only Author and Title

Cluis CP, Mouchel CF, Hardtke CS (2004) The Arabidopsis transcription factor HY5 integrates light and hormone signaling pathways. Plant J 38: 332-347
Pubmed: Author and Title
CrossRef: Author and Title
Google Scholar: Author Only Title Only Author and Title

Duan M, Ma NN, Li D, Deng YS, Kong FY, Lv W, Meng QW (2012) Antisense-mediated suppression of tomato thylakoidal ascorbate

peroxidase influences antioxidant network during chilling stress. Plant Physiol Biochem 58: 37-45
Pubmed: Author and Title
CrossRef: Author and Title
Google Scholar: Author Only Title Only Author and Title

Fillatti JJ, Kiser J, Rose R, Comai L (1987) Efficient transfer of a glyphosate tolerance gene into tomato using a binary Agrobacterium tumefaciens vector. Bio-Technol 5: 726-730
Pubmed: Author and Title
CrossRef: Author and Title
Google Scholar: Author Only Title Only Author and Title

Foyer CH, Neukermans J, Queval G, Noctor G, Harbinson J (2012) Photosynthetic control of electron transport and the regulation of gene expression. J Exp Bot 63: 1637-1661
Pubmed: Author and Title
CrossRef: Author and Title
Google Scholar: Author Only Title Only Author and Title

Foyer CH, Ruban AV, Noctor G (2017) Viewing oxidative stress through the lens of oxidative signalling rather than damage. Biochem J 474: 877-883
Pubmed: Author and Title
CrossRef: Author and Title
Google Scholar: Author Only Title Only Author and Title

Foyer CH, Souriau N, Perret S, Lelandais M, Kunert KJ, Pruvost C, Jouanin L (1995) Overexpression of glutathione reductase but not glutathione synthetase leads to increases in antioxidant capacity and resistance to photoinhibition in poplar trees. Plant Physiol 109: 1047-1057
Pubmed: Author and Title
CrossRef: Author and Title
Google Scholar: Author Only Title Only Author and Title

Franklin KA, Quail PH (2010) Phytochrome functions in Arabidopsis development. J Exp Bot 61: 11-24
Pubmed: Author and Title
CrossRef: Author and Title
Google Scholar: Author Only Title Only Author and Title

Gangappa SN, Botto JF (2016) The multifaceted roles of HY5 in plant growth and development. Mol Plant 9: 1353-1365
Pubmed: Author and Title
CrossRef: Author and Title
Google Scholar: Author Only Title Only Author and Title

Guo ZX, Wang F, Xiang X, Ahammed GJ, Wang MM, Onac E, Zhou J, Xia XJ, Shi K, Yin XR, et al (2016) Systemic induction of photosynthesis via illumination of the shoot apex is mediated by phytochrome B. Plant Physiol 172: 1259-1272
Pubmed: Author and Title
CrossRef: Author and Title
Google Scholar: Author Only Title Only Author and Title

Han H, Gao S, Li B, Dong XC, Feng HL, Meng QW (2010) Overexpression of violaxanthin de-epoxidase gene alleviates photoinhibition of PSII and PSI in tomato during high light and chilling stress. J Plant Physiol 167: 176-183
Pubmed: Author and Title
CrossRef: Author and Title
Google Scholar: Author Only Title Only Author and Title

Hertle AP, Blunder T, Wunder T, Pesaresi P, Pribil M, Armbruster U, Leister D (2013) PGRL1 is the elusive ferredoxin-plastoquinone reductase in photosynthetic cyclic electron flow. Mol Cell 49: 511-523
Pubmed: Author and Title
CrossRef: Author and Title
Google Scholar: Author Only Title Only Author and Title

Jiao Y, Lau OS, Deng XW (2007) Light-regulated transcriptional networks in higher plants. Nat Rev Genet 8: 217-230
Pubmed: Author and Title
CrossRef: Author and Title
Google Scholar: Author Only Title Only Author and Title

Jin H, Liu B, Luo L, Feng D, Wang P, Liu J, Da Q, He Y, Qi K, Wang J, et al (2014) HYPERSENSITIVE TO HIGH LIGHT1 interacts with LOW QUANTUM YIELD OF PHOTOSYSTEM II1 and functions in protection of photosystem II from photodamage in Arabidopsis. Plant Cell 26: 1213-1229
Pubmed: Author and Title
CrossRef: Author and Title
Google Scholar: Author Only Title Only Author and Title

Kasahara M, Kagawa T, Oikawa K, Suetsugu N, Miyao M, Wada M (2002) Chloroplast avoidance movement reduces photodamage in plants. Nature 420: 829-832
Pubmed: Author and Title
CrossRef: Author and Title
Google Scholar: Author Only Title Only Author and Title

Kim HE, Tokura H (1995) Influence of different light intensities during the daytime on evening dressing behavior in the cold. Physiol Behav 58: 779-783
Pubmed: Author and Title
CrossRef: Author and Title
Google Scholar: Author Only Title Only Author and Title

Kingston-Smith AH, Foyer CH (2000) Bundle sheath proteins are more sensitive to oxidative damage than those of the mesophyll in maize leaves exposed to paraquat or low temperatures. J Expt Bot 51: 123-130
Pubmed: Author and Title
CrossRef: Author and Title
Google Scholar: Author Only Title Only Author and Title

Kingston-Smith AH, Harbinson J, Williams J, Foyer CH (1997) Effect of chilling on carbon assimilation, enzyme activation, and photosynthetic electron transport in the absence of photoinhibition in maize leaves. Plant Physiol 114: 1039-1046
Pubmed: Author and Title
CrossRef: Author and Title
Google Scholar: Author Only Title Only Author and Title

Klughammer C, Schreiber U (2008) Saturation pulse method for assessment of energy conversion in PSI. PAM Application Notes 1: 11-14
Pubmed: Author and Title
CrossRef: Author and Title
Google Scholar: Author Only Title Only Author and Title

Kromdijk J, Głowacka K, Leonelli L, Gabilly ST, Iwai M, Niyogi KK, Long SP (2016) Improving photosynthesis and crop productivity by accelerating recovery from photoprotection. Science 354: 857-861
Pubmed: Author and Title
CrossRef: Author and Title
Google Scholar: Author Only Title Only Author and Title

Lau OS, Deng XW (2010) Plant hormone signaling lightens up: integrators of light and hormones. Curr Opin Plant Biol 13: 571-577
Pubmed: Author and Title
CrossRef: Author and Title
Google Scholar: Author Only Title Only Author and Title

Lei Y, Lu L, Liu HY, Li S, Xing F, Chen LL (2014) CRISPR-P: A web tool for synthetic single-guide RNA design of CRISPR-system in plants. Mol Plant 7: 1494-1496
Pubmed: Author and Title
CrossRef: Author and Title
Google Scholar: Author Only Title Only Author and Title

Li XP, Mullermoule P, Gilmore AM, Niyogi KK (2002) PsbS-dependent enhancement of feedback de-excitation protects photosystem II from photoinhibition. Proc Natl Acad Sci USA 99: 15222-15227
Pubmed: Author and Title
CrossRef: Author and Title
Google Scholar: Author Only Title Only Author and Title

Li ZF, Zhang LX, Yu YW, Quan RD, Zhang ZJ, Zhang HW, Huang RF (2011) The ethylene response factor AtERF11 that is transcriptionally modulated by the bZIP transcription factor HY5 is a crucial repressor for ethylene biosynthesis in Arabidopsis. Plant J 68: 88-99
Pubmed: Author and Title
CrossRef: Author and Title
Google Scholar: Author Only Title Only Author and Title

Liu J, Last RL (2015) A land plant-specific thylakoid membrane protein contributes to photosystem II maintenance in Arabidopsis thaliana. Plant J 82: 731-743
Pubmed: Author and Title
CrossRef: Author and Title
Google Scholar: Author Only Title Only Author and Title

Liu Y, Roof S, Ye Z, Barry C, van Tuinen A, Vrebalov J, Bowler C, Giovannoni J (2004) Manipulation of light signal transduction as a means of modifying fruit nutritional quality in tomato. Proc Natl Acad Sci USA 101: 9897-9902
Pubmed: Author and Title
CrossRef: Author and Title
Google Scholar: Author Only Title Only Author and Title

Liu YL, Schiff M, Dinesh-Kumar SP (2002) Virus-induced gene silencing in tomato. Plant J 31:777-786
Pubmed: Author and Title
CrossRef: Author and Title
Google Scholar: Author Only Title Only Author and Title

Livak KJ, Schmittgen TD (2001) Analysis of relative gene expression data using real-time quantitative PCR and the 2-ΔΔΔCTmethod. Methods 25: 402-408
Pubmed: Author and Title
CrossRef: Author and Title

Google Scholar: Author Only Title Only Author and Title

Maruta T, Tanouchi A, Tamoi M, Yabuta Y, Yoshimura K, Ishikawa T, Shigeoka S (2010) Arabidopsis chloroplastic ascorbate peroxidase isoenzymes play a dual role in photoprotection and gene regulation under photooxidative stress. Plant Cell Physiol 51: 190-200
Pubmed: Author and Title
CrossRef: Author and Title
Google Scholar: Author Only Title Only Author and Title

Mittal A, Gampala SSL, Ritchie GL, Payton P, Burke JJ, Rock CD (2014) Related to ABA-insensitive 3 (ABI3)/Viviparous 1 and AtABI5 transcription factor coexpression in cotton enhances drought stress adaptation. Plant Biotechnol J 12: 578-589
Pubmed: Author and Title
CrossRef: Author and Title
Google Scholar: Author Only Title Only Author and Title

Möglich A, Yang X, Ayers RA, Moffat K (2010) Structure and function of plant photoreceptors. Annu Rev Plant Biol 61: 21-47
Pubmed: Author and Title
CrossRef: Author and Title
Google Scholar: Author Only Title Only Author and Title

Munekage Y, Hashimoto M, Miyake C, Tomizawa KI, Endo T, Tasaka M, Shikanai T (2004) Cyclic electron flow around photosystem I is essential for photosynthesis. Nature 429: 579-582
Pubmed: Author and Title
CrossRef: Author and Title
Google Scholar: Author Only Title Only Author and Title

Munekage Y, Hojo M, Meurer J, Endo T, Tasaka M, Shikanai T (2002) PGR5 is involved in cyclic electron flow around photosystem I and is essential for photoprotection in Arabidopsis. Cell 110: 361-371
Pubmed: Author and Title
CrossRef: Author and Title
Google Scholar: Author Only Title Only Author and Title

Murata Y, Pei ZM, Mori IC, Schroeder JI (2001) Abscisic acid activation of plasma membrane Ca2+ channels in guard cells requires cytosolic NADPH and is differentially disrupted upstream and downstream of reactive oxygen species production in abi1-1 and abi2-1 protein phosphatase 2C mutants. Plant Cell 13: 2513-2523
Pubmed: Author and Title
CrossRef: Author and Title
Google Scholar: Author Only Title Only Author and Title

Nagata Nagata M, Yamamoto N, Shigeyama T, Terasawa Y, Anai T, Sakai T, Inada S, Arima S, Hashiguchi M, Akashi R, et al (2015) Red/Far red light controls arbuscular mycorrhizal colonization via jasmonic acid and strigolactone signaling. Plant Cell Physiol 56: 2100-2109
Pubmed: Author and Title
CrossRef: Author and Title
Google Scholar: Author Only Title Only Author and Title

Nashilevitz S, Melamed-Bessudo C, Izkovich Y, Rogachev I, Osorio S, Itkin M, Adato A, Pankratov I, Hirschberg J, Fernie AR, et al (2010) An orange ripening mutant links plastid NAD(P)H dehydrogenase complex activity to central and specialized metabolism during tomato fruit maturation. Plant Cell 22: 1977-1997
Pubmed: Author and Title
CrossRef: Author and Title
Google Scholar: Author Only Title Only Author and Title

Nishiyama Y, Allakhverdiev SI, Murata N (2006) A new paradigm for the action of reactive oxygen species in the photoinhibition of photosystem II. Biochim Biophys Acta 1757: 742-749
Pubmed: Author and Title
CrossRef: Author and Title
Google Scholar: Author Only Title Only Author and Title

Niyogi KK, Björkman O, Grossman AR (1997) The roles of specific xanthophylls in photoprotection. Proc Natl Acad Sci USA 94: 14162-14167
Pubmed: Author and Title
CrossRef: Author and Title
Google Scholar: Author Only Title Only Author and Title

Niyogi KK, Grossman AR, Björkman O (1998) Arabidopsis mutants define a central role for the xanthophyll cycle in the regulation of photosynthetic energy conversion. Plant Cell 10: 1121-1134
Pubmed: Author and Title
CrossRef: Author and Title
Google Scholar: Author Only Title Only Author and Title

Okegawa Y, Kagawa Y, Kobayashi Y, Shikanai T (2008) Characterization of factors affecting the activity of photosystem I cyclic electron transport in chloroplasts. Plant Cell Physiol 49: 825-834
Pubmed: Author and Title
CrossRef: Author and Title
Google Scholar: Author Only Title Only Author and Title

Osterlund MT, Hardtke CS, Wei N, Deng XW (2000) Targeted destabilization of HY5 during light-regulated development of Arabidopsis. Nature 405: 462-466
Pubmed: Author and Title
CrossRef: Author and Title
Google Scholar: Author Only Title Only Author and Title

Pan CT, Ye L, Qin L, Liu X, He YJ, Wang J, Chen LF, Lu G (2016) CRISPR/Cas9-mediated efficient and heritable targeted mutagenesis in tomato plants in the first and later generations. Sci Rep 6: 24765
Pubmed: Author and Title
CrossRef: Author and Title
Google Scholar: Author Only Title Only Author and Title

Petroutsos D, Tokutsu R, Maruyama S, Flori S, Greiner A, Magneschi L, Cusant L, Kottke T, Mittag M, Hegemann P, et al (2016) A blue-light photoreceptor mediates the feedback regulation of photosynthesis. Nature 537:563-566
Pubmed: Author and Title
CrossRef: Author and Title
Google Scholar: Author Only Title Only Author and Title

Porra RJ, Thompson WA, Kriedemann PE (1989) Determination of accurate extinction coefficients and simultaneous equations for assaying chlorophylls a and b extracted with four different solvents: Verification of the concentration of chlorophyll standards by atomic absorption spectroscopy. Biochim Biophys Acta 975: 384-394
Pubmed: Author and Title
CrossRef: Author and Title
Google Scholar: Author Only Title Only Author and Title

Quail PH (2002a) Phytochrome photosensory signalling networks. Nat Rev Mol Cell Biol 3: 85-93
Pubmed: Author and Title
CrossRef: Author and Title
Google Scholar: Author Only Title Only Author and Title

Quail PH (2002b) Photosensory perception and signalling in plant cells: new paradigms? Curr Opin Cell Biol 14: 180-188
Pubmed: Author and Title
CrossRef: Author and Title
Google Scholar: Author Only Title Only Author and Title

Ruban AV, Berera R, Ilioaia C, van Stokkum IHM, Kennis JTM, Pascal AA, van Amerongen H, Robert B, Horton P, van Grondelle R (2007) Identification of a mechanism of photoprotective energy dissipation in higher plants. Nature 450: 575-578
Pubmed: Author and Title
CrossRef: Author and Title
Google Scholar: Author Only Title Only Author and Title

Sasidharan R, Chinnappa CC, Voesenek LACJ, Pierik R (2009) A molecular basis for the physiological variation in shade avoidance responses. Plant Signal Behav 4: 528-529
Pubmed: Author and Title
CrossRef: Author and Title
Google Scholar: Author Only Title Only Author and Title

Shikanai T (2007) Cyclic electron transport around photosystem I: genetic approaches. Annu Rev Plant Biol 58: 199-217
Pubmed: Author and Title
CrossRef: Author and Title
Google Scholar: Author Only Title Only Author and Title

Strand DD, Livingston AK, Satoh-Cruz M, Froehlich JE, Maurino VG, Kramer DM (2015) Activation of cyclic electron flow by hydrogen peroxide in vivo. Proc Natl Acad Sci USA 112: 5539-5544
Pubmed: Author and Title
CrossRef: Author and Title
Google Scholar: Author Only Title Only Author and Title

Takahashi S, Badger MR (2011) Photoprotection in plants: a new light on photosystem II damage. Trends Plant Sci 16: 53-60
Pubmed: Author and Title
CrossRef: Author and Title
Google Scholar: Author Only Title Only Author and Title

Takahashi S, Milward SE, Fan DY, Chow WS, Badger MR (2009) How does cyclic electron flow alleviate photoinhibition in Arabidopsis? Plant Physiol 149: 1560-1567
Pubmed: Author and Title
CrossRef: Author and Title
Google Scholar: Author Only Title Only Author and Title

Wang F, Guo ZX, Li HZ, Wang MM, Onac E, Zhou J, Xia XJ, Shi K, Yu JQ, Zhou YH (2016) Phytochrome A and B function antagonistically to regulate cold tolerance via abscisic acid-dependent jasmonate signaling. Plant Physiol 170: 459-471
Pubmed: Author and Title
CrossRef: Author and Title
Google Scholar: Author Only Title Only Author and Title

Xia XJ, Gao CJ, Song LX, Zhou YH, Shi K, Yu JQ (2014) Role of H2O2 dynamics in brassinosteroid-induced stomatal closure and opening in Solanum lycopersicum. Plant Cell Environ 37: 2036-2050
Pubmed: Author and Title
CrossRef: Author and Title
Google Scholar: Author Only Title Only Author and Title

Xia XJ, Wang YJ, Zhou YH, Tao Y, Mao WH, Shi K, Asami T, Chen ZX, Yu JQ (2009) Reactive oxygen species are involved in brassinosteroid-induced stress tolerance in cucumber. Plant Physiol 150: 801-814
Pubmed: Author and Title
CrossRef: Author and Title
Google Scholar: Author Only Title Only Author and Title

Xie XZ, Xue YJ, Zhou JJ, Zhang B, Chang H, Takano M (2011) Phytochromes regulate SA and JA signaling pathways in rice and are required for developmentally controlled resistance to Magnaporthe grisea. Mol Plant 4: 688-696
Pubmed: Author and Title
CrossRef: Author and Title
Google Scholar: Author Only Title Only Author and Title

Xing Y, Jia W, Zhang J (2008) AtMKK1 mediates ABA-induced CAT1 expression and H2O2 production via AtMPK6-coupled signaling in Arabidopsis. Plant J 54: 440-451
Pubmed: Author and Title
CrossRef: Author and Title
Google Scholar: Author Only Title Only Author and Title

Xu CJ, Fraser PD, Wang WJ, Bramley PM (2006) Differences in the carotenoid content of ordinary citrus and lycopene-accumulating mutants. J Agric Food Chem 54: 5474-5481
Pubmed: Author and Title
CrossRef: Author and Title
Google Scholar: Author Only Title Only Author and Title

Xu D, Li J, Gangappa SN, Hettiarachchi C, Lin F, Andersson MX, Jiang Y, Deng XW, Holm M (2014) Convergence of light and ABA signaling on the ABI5 promoter. PLoS Genet 10: e1004197
Pubmed: Author and Title
CrossRef: Author and Title
Google Scholar: Author Only Title Only Author and Title

Yamori W, Makino A, Shikanai T (2016) A physiological role of cyclic electron transport around photosystem I in sustaining photosynthesis under fluctuating light in rice. Sci Rep 6: 20147
Pubmed: Author and Title
CrossRef: Author and Title
Google Scholar: Author Only Title Only Author and Title

Yi C, Deng XW (2005) COP1 from plant photomorphogenesis to mammalian tumorigenesis. Trends Cell Biol 15: 618-625
Pubmed: Author and Title
CrossRef: Author and Title
Google Scholar: Author Only Title Only Author and Title

de Wit M, Spoel SH, Sanchez-Perez GF, Gommers CMM, Pieterse CMJ, Voesenek LACJ, Pierik R (2013) Perception of low red:far-red ratio compromises both salicylic acid- and jasmonic acid-dependent pathogen defences in Arabidopsis. Plant J 75: 90-103
Pubmed: Author and Title
CrossRef: Author and Title
Google Scholar: Author Only Title Only Author and Title

Zhang AY, Jiang MY, Zhang JH, Ding HD, Xu SC, Hu XL, Tan MP (2007) Nitric oxide induced by hydrogen peroxide mediates abscisic acid-induced activation of the mitogen-activated protein kinase cascade involved in antioxidant defense in maize leaves. New Phytol 175: 36-50
Pubmed: Author and Title
CrossRef: Author and Title
Google Scholar: Author Only Title Only Author and Title

Zhao Y, Chan Z, Xing L, Liu XD, Hou YJ, Chinnusamy V, Wang P, Duan C, Zhu JK (2013) The unique mode of action of a divergent member of the ABA-receptor protein family in ABA and stress signaling. Cell Res 23: 1380-1395
Pubmed: Author and Title
CrossRef: Author and Title
Google Scholar: Author Only Title Only Author and Title

Zhou J, Wang J, Li X, Xia XJ, Zhou YH, Shi K, Chen ZX, Yu JQ (2014) H2O2 mediates the crosstalk of brassinosteroid and abscisic acid in tomato responses to heat and oxidative stresses. J Exp Bot 65: 4371-4383
Pubmed: Author and Title
CrossRef: Author and Title
Google Scholar: Author Only Title Only Author and Title

Zhou J, Wang J, Shi K, Xia XJ, Zhou YH, Yu JQ (2012) Hydrogen peroxide is involved in the cold acclimation-induced chilling tolerance of tomato plants. Plant Physiol Biochem 60: 141-149
Pubmed: Author and Title

CrossRef: Author and Title
Google Scholar: Author Only Title Only Author and Title

Zhu J, Dong CH, Zhu JK (2007) Interplay between cold-responsive gene regulation, metabolism and RNA processing during plant cold acclimation. Curr Opin Plant Biol 10: 290-295

Pubmed: Author and Title
CrossRef: Author and Title
Google Scholar: Author Only Title Only Author and Title